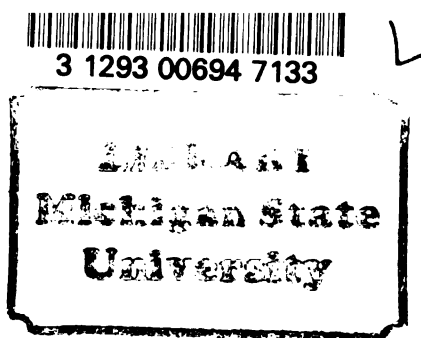


THESIS



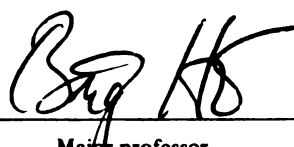
This is to certify that the  
thesis entitled

ACOUSTIC ATTENUATION AND IMPEDANCE CHARACTERIZATION  
BY BI-DIRECTIONAL IMPULSE RESPONSE TECHNIQUE  
presented by

M.A. Anura P. Jayasumana

has been accepted towards fulfillment  
of the requirements for

MASTERS degree in SCIENCE

  
\_\_\_\_\_  
Major professor

Date 12 th May 1982



RETURNING MATERIALS:  
Place in book drop to  
remove this checkout from  
your record. FINES will  
be charged if book is  
returned after the date  
stamped below.

AUG 08 1997

--	--	--

ACOUSTIC ATTENUATION AND IMPEDANCE CHARACTERIZATION  
BY BI-DIRECTIONAL IMPULSE RESPONSE TECHNIQUE

By

M.A. Anura P. Jayasumana

A THESIS

Submitted to  
Michigan State University  
in partial fulfilment of the requirements  
for the degree of

MASTER OF SCIENCE

Department of Electrical Engineering  
and System Science

1982

6-117641



## ABSTRACT

### ACOUSTIC ATTENUATION AND IMPEDANCE CHARACTERIZATION BY BI-DIRECTIONAL IMPULSE RESPONSE TECHNIQUE

By

M.A. Anura P. Jayasumana

This thesis presents an investigation into the use of ultrasound reflection techniques for attenuation and impedance imaging. For this purpose, the object to be imaged is modelled in one of the following two forms. First the object is assumed to consist of parallel homogeneous layers. Second, the object is made of an inhomogeneous medium, which does not contain any discontinuities in impedance. Expressions relating the impulse response functions with the attenuation coefficient and impedance have been derived. The theoretical development for a layered structure has been verified by experiments. The results of the experiments are presented. The method outlined in this thesis yields the variation of the impedance and the attenuation coefficient inside the object. To obtain this information, the object has to be interrogated from opposite sides using an ultrasonic pulse.

TO MOTHER AND FATHER

## ACKNOWLEDGMENTS

The author extends his greatest gratitude to Dr. Bong Ho, his thesis advisor, who has been a constant source of guidance and support. Sincere appreciation is expressed to Dr. Ray Nettleton for his review and suggestions to this thesis. Appreciation is also extended to Dr. R. Zapp, a member of the guidance committee, for his suggestions to this thesis. A very special thanks is extended to Geetha Jayasumana for her help and support.

## TABLE OF CONTENTS

	Page
LIST OF TABLES	v
LIST OF FIGURES	vi
I. INTRODUCTION	1
1.1 Basic principles of ultrasound propagation	3
1.2 Previous work	12
II. THEORETICAL CONSIDERATIONS	16
2.1 Reflections from a layered structure	16
2.2 Reflections from an arbitrary impedance profile	20
2.3 Improvement of the accuracy of the impulse response function	25
III. ATTENUATION VARIATION FROM REFLECTED SIGNALS	31
3.1 Relationship of attenuation to impulse response function of a layered object	31
3.2 Relationship of attenuation to impulse response function of an inhomogeneous medium	36
IV. EXPERIMENTAL PROCEDURE AND RESULTS	42
4.1 Data collection	42
4.2 Data processing	44
4.3 Experimental results	48
V. CONCLUSION	68
APPENDIX A	72
APPENDIX B	74
APPENDIX C	76
BIBLIOGRAPHY	78

## LIST OF TABLES

	Page
TABLE 1.1 Propagation velocities in some biological materials	4
TABLE 1.2 Characteristic impedance of some biological materials	5
TABLE 1.3 Biological attenuation coefficients	11
TABLE 4.1 Results for test object 1 - using direct i.r.f.	55
TABLE 4.2 Results for test object 1 - using restored i.r.f.	56
TABLE 4.3 Layer parameters for test object 1 from direct measurements	57
TABLE 4.4 Results for test object 2 - using direct i.r.f. and $r_1 = a_1$	61
TABLE 4.5 Results for test object 2 - using direct i.r.f. and $r_6 = -b_6$	62
TABLE 4.6 Results for test object 2 - using restored i.r.f. and $r_1 = a_1$	63
TABLE 4.7 Results for test object 2 - using restored i.r.f. and $r_6 = -b_6$	64
TABLE 4.8 Results for test object 2 - using direct i.r.f.	65
TABLE 4.9 Results for test object 2 - using restored i.r.f.	66
TABLE 4.10 Layer parameters for test object 2. from direct measurements	67

## LIST OF FIGURES

FIGURE 1.1	Reflection and transmission of acoustic wave	6
FIGURE 2.1	A one dimensional layered structure	17
FIGURE 2.2	First and second order reflections from a layered structure	19
FIGURE 2.3	A one dimensional inhomogeneous structure	20
FIGURE 2.4	Frequency spectrum of a typical incident wave	26
FIGURE 2.5	Spectral extrapolation for impulse response function improvement	29
FIGURE 3.1	Bi-directional ultrasonic interrogation	32
FIGURE 3.2	A layered structure	32
FIGURE 3.3	An inhomogeneous medium	37
FIGURE 3.4	Time relationships for bi-directional ultrasonic interrogation	37
FIGURE 4.1	Incident waveform recording	43
FIGURE 4.2	Reflected waveform recording	43
FIGURE 4.3	Bi-directional impulse response functions of a layered object	43
FIGURE 4.4	Test object 1	49
FIGURE 4.5	Incident waveform	50
FIGURE 4.6	Incident spectrum and the Hanning filter	51
FIGURE 4.7	Reflected waveform	52
FIGURE 4.8	Direct impulse response function of test object 1 - before and after amplitude detection	53

FIGURE 4.9	Frequency restored impulse response function of test object 1	54
FIGURE 4.10	Test object 2	57
FIGURE 4.11	Bi-directional direct impulse response function of test object 2	59
FIGURE 4.12	Bi-directional frequency restored impulse response functions of test object 2	60
FIGURE A.1	Flow diagram of the amplitude detection scheme	77

## CHAPTER I

### INTRODUCTION

Use of ultrasound for biomedical imaging purposes has been under investigation for more than three decades. Propagation of ultrasound in biological material depends on the ultrasound propagation velocity, the acoustic impedance, the attenuation in the tissue and the scattering of ultrasound by the inhomogeneities in the tissue structure. In contrast, propagation of X-ray in tissue depends only on the density of the tissue. Thus it appears that there is a considerable amount of information contained in an ultrasonic wave propagated through a tissue. This coupled with the noninvasive nature of ultrasound has been its main attraction in biomedical applications.

In general, a biomedical ultrasonic imaging system will transmit an acoustic pulse in the frequency range of 1-10 MHz through the object under investigation and receive a waveform which is a result of the transmitted wave interacting with the object. In transmission techniques, the received signal is the deformed pulse resulting from the incident pulse propagating through the object. In reflection techniques the received signal is the waveform resulting from reflections of the incident pulse at the discontinuities inside the object. Until recently, only the amplitude information of the received signal was used for imaging. During the last decade, research has been conducted on how to use the frequency and phase information of the received signal for imaging and tissue characterization.



Ultrasonic impediography was a result of this. It allows the determination of the acoustic impedance of the medium along the path of propagation.

This thesis investigates a method which would allow extration of information about the variation of acoustical attenuation in addition to the variation of acoustical impedance along the path of propagation. In certain physiological structures, knowledge of attenuation may be more important than the knowledge of impedance. For example, the impedance transition between gray and white brain matter is only about 0.1%, whereas the corresponding change in acoustical attenuation is two orders of magnitude larger<sup>15</sup>.

First, the basic properties of ultrasound propagation will be briefly reviewed. Second, the basic principles of ultrasonic impediography and range resolution improvement will be outlined. Third, it will be shown that information sufficient to find out the variation of attenuation along the path of propagation can be extracted by transmitting two ultrasound signals from opposite sides of the specimen. For this purpose, the object is modelled in one of the following two ways. It can be modelled as consisting of parallel layers of different impedances<sup>1</sup>. Certain biological materials however cannot be represented by distinct boundaries. In such a case, the acoustic impedance is assumed to vary continuously along the path of propagation. Any discontinuity has to be handled by a combination of the two models. Experimental results are presented to show the validity of the theoretical development. The limitations and the means by which this method can be improved are also discussed.

Next two sections of this chapter will review the basic properties of ultrasound propagation and present the state-of-the-art in ultrasonic imaging and tissue characterization research.

### 1.1 BASIC PRINCIPLES OF ULTRASOUND PROPAGATION

The propagation of ultrasound in biological matter is due mainly to the longitudinal waves, i.e. direction of propagation of the wave is the same as the direction of vibration of particles. The propagation due to shear waves can be neglected because the attenuation coefficient for shear waves is extremely high<sup>6</sup>.

The wave motion in a lossless medium can be described by

$$\nabla^2 p - \frac{1}{c^2} \frac{\partial^2 p}{\partial t^2} = 0 \quad (1.1.1)$$

and

$$c = \sqrt{\frac{K_a}{\rho}} = \sqrt{\frac{1}{k\rho}} \quad (1.1.2)$$

where

- $p$  = pressure
- $c$  = group velocity of the ultrasound wave
- $K_a$  = adiabatic bulk modulus of the material
- $k$  = adiabatic compressibility of the material
- $\rho$  = density of the material.

In one dimension, equation (1.1.1) becomes

$$\frac{\partial^2 p}{\partial t^2} = c^2 \frac{\partial^2 p}{\partial x^2} \quad (1.1.3)$$

The general solution to this equation is given by,

$$p = f(x-ct) + f'(x+ct) \quad (1.1.4)$$

where  $f(x-ct)$  and  $f'(x+ct)$  are forward and backward travelling waves respectively. Some basic properties of ultrasound propagation will be considered now.

#### Acoustic velocity:

It has been found that the velocity of propagation,  $c$ , of ultrasound in biological matter has only a small dispersion, i.e. it is independent of the frequency for most practical purposes<sup>25</sup>. The velocity in one kind of soft tissue is almost the same as that in another. But the velocity in bones is much faster than that in the tissue. The velocity is also a function of the temperature. Propagation properties of some biological materials are given in Table 1.1.

TABLE 1.1 Propagation velocities in some biological materials\*.

Tissue	Mean velocity (m/s)
Fat	1450
Human tissue, mean value	1540
Brain	1541
Liver	1549
Kidney	1561
Spleen	1566
Blood	1570
Muscle	1585
Skull-bone	4089

\* From P.N.T.Wells<sup>25</sup>.

Characteristic impedance :

The characteristic impedance of a medium is defined as the ratio of the pressure to the phase velocity associated with the propagation of the acoustic waves. It is given by,

$$\underline{Z} = \left[ \frac{\underline{p}}{k} \right]^{\frac{1}{2}} = \underline{\rho c} \quad (1.1.5)$$

The characteristic impedance of the medium may be complex<sup>11</sup>. For biological matter however, the imaginary part is negligible<sup>25</sup>.

$$\text{Thus } p = Zv \quad (1.1.6)$$

where  $p$  = pressure

$v$  = phase velocity or the velocity of particle vibration

$Z$  = characteristic impedance of the medium.

Characteristic impedances of few biological material are given in Table 1.2.

TABLE 1.2 Characteristic impedance of some biological materials\*.

Tissue	$Z \text{ (g/cm}^2\text{.s) } \times 10^{-5}$
Fat	1.38
Brain	1.58
Kidney	1.62
Human tissue, mean value	1.63
Spleen	1.64
Liver	1.65
Muscle	1.70
Skull-bone	7.80

\* From P.N.T.Wells<sup>25</sup>.

### Reflection and refraction at plane surfaces :

When an ultrasonic plane wave strikes the boundary between two different media, it may be partially reflected as shown in Figure 1.1. If the dimensions of the reflecting object are large compared to the acoustic wave length, the geometrical laws of reflection apply. If the wavelength is comparable with linear dimensions of the reflecting object, these laws cease to apply and diffraction occurs. Assume the case where the wavelength is small compared to the dimensions of the reflector.

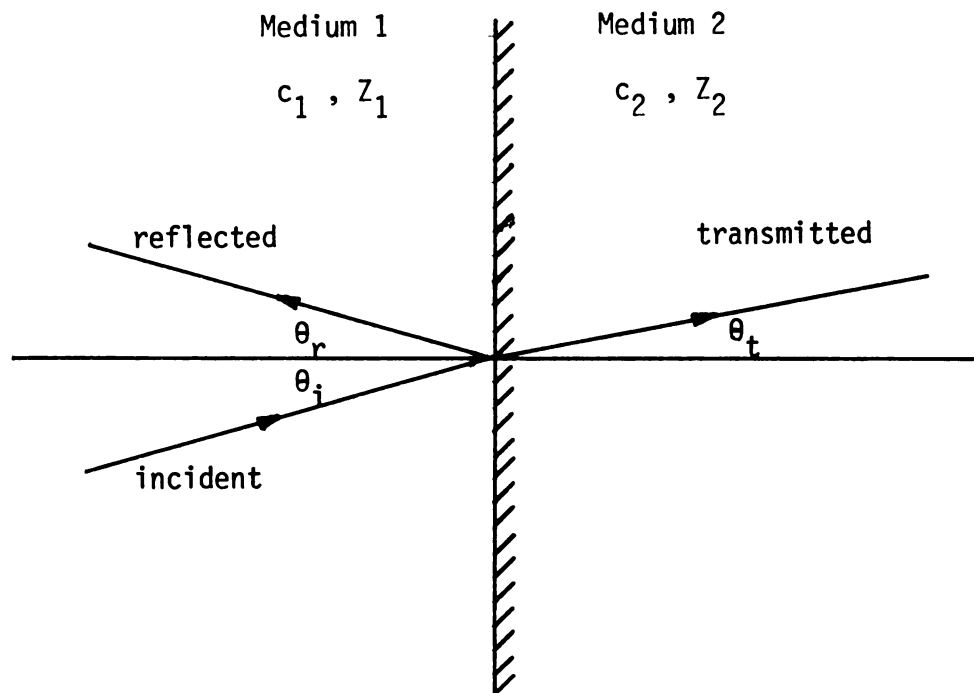


FIGURE 1.1 Reflection and transmission of acoustic wave

By Snell's law,

$$\theta_i = \theta_r \quad (1.1.7)$$

$$\frac{\sin \theta_i}{\sin \theta_t} = \frac{c_1}{c_2} \quad (1.1.8)$$

where

$c_1$  = acoustic velocity in medium 1

$c_2$  = acoustic velocity in medium 2

$\theta_i$  = angle of incident wave

$\theta_r$  = angle of reflected wave

$\theta_t$  = angle of transmitted wave

The following boundary conditions apply.

1. The total pressure on each side of the boundary must be equal.
2. The particle velocity on each side of the boundary must be continuous.

Hence,

$$p_i + p_r = p_t \quad (1.1.9)$$

$$v_i \cos \theta_i - v_r \cos \theta_r = v_t \cos \theta_t \quad (1.1.10)$$

where

$p_i$  = acoustic pressure of the incident wave

$p_r$  = acoustic pressure of the reflected wave

$p_t$  = acoustic pressure of the transmitted wave

$v_i$  = particle velocity of the incident wave

$v_r$  = particle velocity of the reflected wave

$v_t$  = particle velocity of the transmitted wave.

From the definition of the acoustic impedance, equation (1.1.6),

$$p_i = Z_1 v_i \quad (1.1.11)$$

$$p_r = Z_1 v_r \quad (1.1.12)$$

$$p_t = Z_2 v_t \quad (1.1.13)$$

where

$$Z_1 = \text{acoustic impedance of the first medium}$$

$$Z_2 = \text{acoustic impedance of the second medium.}$$

From equations (1.1.7) - (1.1.13),

$$r = \frac{p_r}{p_i} = \frac{Z_2 \cos \theta_i - Z_1 \cos \theta_t}{Z_2 \cos \theta_i + Z_1 \cos \theta_t} \quad (1.1.14)$$

$$\tau = \frac{p_t}{p_i} = \frac{2 Z_2 \cos \theta_i}{Z_2 \cos \theta_i + Z_1 \cos \theta_t} \quad (1.1.15)$$

The reflectivity,  $r$  is defined as the ratio of pressure reflected to the pressure incident and the transmissivity,  $\tau$  as the ratio of pressure transmitted to the pressure of the incident wave.

For normal incidence,

$$\theta_i = \theta_r = \theta_t = 0 \quad (1.1.16)$$

Thus from equations (1.1.14) and (1.1.15), the reflection coefficient  $r$  is

$$r = \frac{p_r}{p_i} = \frac{Z_2 - Z_1}{Z_2 + Z_1} \quad (1.1.17)$$

and the transmissivity is

$$\tau = \frac{p_t}{p_i} = \frac{2 Z_2}{Z_2 + Z_1} \quad (1.1.18)$$

The intensity reflection coefficient  $\Gamma_r$  and the intensity transmission coefficient  $\Gamma_t$  are given by,

$$\Gamma_r = \left[ \frac{p_r}{p_i} \right]^2 = \left[ \frac{Z_2 \cos \theta_i - Z_1 \cos \theta_t}{Z_2 \cos \theta_i + Z_1 \cos \theta_t} \right]^2 \quad (1.1.19)$$

$$\Gamma_t = \left[ \frac{p_t}{p_i} \right]^2 \cdot \frac{Z_1}{Z_2} = \frac{4 Z_1 Z_2 \cos^2 \theta_i}{(Z_2 \cos \theta_i + Z_1 \cos \theta_t)^2} \quad (1.1.20)$$

From equations (1.1.17) and (1.1.18),

$$\frac{p_t}{p_i} = 1 + \frac{p_r}{p_i} \quad (1.1.21)$$

Ultrasonic attenuation :

Attenuation of ultrasound in matter may be due to the combined effect of several different mechanisms<sup>25</sup>. In certain situations however, a certain mechanism may predominate. One of the mechanisms is the result of deviation of the beam from a parallel beam.

Another is due to scattering by elastic discontinuities within the medium. A discontinuity acts as a reflecting surface, the size of which determines its effect as a scatterer. The scattered energy will no longer propagate in the original direction, thus causing attenuation. The attenuation due to absorption causes the acoustical energy to be converted to some other form of energy, typically heat. When an adiabatic stress and the resulting strain are not related in a linear manner, a non-viscous mechanism occurs, in which the dissipation of energy is proportional to the strain, rather than the rate of change of strain. The loss of energy is constant for each cycle, and hence the elastic hysteresis attenuation is proportional to the frequency of the ultrasound wave.



The attenuation in fluids mainly depends on the viscosity and the heat conduction. The motion of particles is opposed by the viscosity of the medium and this causes generation of heat. If the heat conduction is significant, thermal energy may also move in space. The time lag between the pressure and the density of the medium is controlled by the time required for the viscous stress to be equalized, or for the heat conduction to occur from high to low pressure regions of ultrasonic field. This time lag accounts for the energy absorption<sup>25</sup>.

Energy can exist in a medium in different forms such as molecular vibrational energy, translational energy, lattice vibrational energy and so on. In the presense of an ultrasonic wave, there can be an increase in energy in one or more of these forms. This mechanism, called relaxation, can cause absorption of acoustical energy. This form of attenuation is related to the frequency in a nonlinear manner.

No general theory of absorption seem to be possible for biological materials<sup>25</sup>. But it is characterized experimentally by the relation

$$I = I_0 \exp( -2\alpha(f)d ) \quad (1.1.22)$$

where

$I$  = intensity of the acoustic beam after it has passed through a distance  $d$

$I_0$  = initial intensity of the acoustic beam

$d$  = distance travelled through the medium

$\alpha(f)$  = attenuation coefficient characteristic of the medium.

The factor 2 in the exponent accounts for the fact that the intensity is proportional to the square of the pressure. For biological material in general<sup>21</sup>,

$$\alpha(f) = \alpha_0 f \quad (1.1.23)$$

where

$\alpha_0$  = attenuation per unit distance at 1 MHz

$f$  = frequency of the acoustic wave in MHz.

Attenuation coefficients of some biological material are given in Table 1.3.

TABLE 1.3 Biological attenuation coefficients

Tissue	Attn. coefficient Np/cm.MHz	Temp. °C	Frequency MHz
Liver, Human*	.135	body	1.5
Liver, Human*	.143	40	0.97
Liver, Porcine*	.136	25	4.0
Spleen, Human*	.058	18	1.6
Fat, Human*	.069	37	1.0
Abdominal wall, Human*	.074	-	1.0
Brain (average), Human@	.11	37	1.0
Cortical gray matter, Cat@	.08	37	1.0
Cortical white matter, Cat@	.14	37	1.0

\* From comprehensive compilation of empherical ultrasonic properties of Mammalian tissue<sup>10</sup>.

@ From Biological Engineering<sup>24</sup>.

## 1.2 PREVIOUS WORK

In recent years, a number of techniques have been developed to extract information about biological objects from ultrasonic signals which have interacted with the object. These techniques make use of the frequency and phase information in addition to the amplitude information available in the received signal.

Ultrasonic impediography is based on the time domain characterization of the object in terms of an impulse response function. This approach utilizes amplitude, frequency and phase information available in the received signal. Jones<sup>12-14</sup> has used the incident and reflected signals to obtain the object impulse response function which was then integrated to give the impedance variation along the path of propagation. In addition Jones has also derived the relationships between the impulse response function and the impedance variation for different lossless structures in the presence and the absence of multiple reflections<sup>12</sup>.

Accurate determination of the impulse response function plays a critical role in impediography. The conventional approach is to deconvolve the incident and reflected signals to obtain the impulse response function. However, due to the finite bandwidth of the transducer, only a small band of frequency components of the impulse response function can be accurately determined. This limits the range resolution as well as the accuracy in amplitude of the impulse response function. Several methods have been developed to overcome this limitation. Papoulis, et al.<sup>23</sup> describes a method in which the reliable frequency components of the impulse response function are first used to make an initial estimate of the peak values, and the

epoch times. These values are then used to estimate the out of band or unreliable frequency components. This method is further discussed in section 2.3.1 of this thesis.

Kuc, et al.<sup>17</sup> outline a Kalman filtering approach to this problem. The Kalman filter processes the observed time samples to predict the next sample value. The error between the predicted value and the value actually observed is due either to the presense of noise or due to a reflector.

Papoulis, et al.<sup>22</sup> have demonstrated another method to improve the range resolution of an impulse response function by spectral extrapolation. This takes into account the fact that the impulse response function has a finite time duration and hence in the frequency domain it has a large bandwidth. First they use only the reliable section of the transfer function to obtain the impulse response function. This would yield a signal having a large duration in the time domain. It is truncated to the known impulse response function duration, and this can now be used to estimate the other frequency components of the transfer function. It has been shown that after a number of iterations, the result approaches the actual impulse response function, even in the presense of considerable noise. This method is discussed in detail in section 2.3.2 of this thesis.

Beretsky, et al.<sup>1-4</sup> have made use of the processing techniques mentioned above in their research work. They have obtained the impedigrams of nonbiological as well as biological structures with considerable success.

Fourcade, et al.<sup>5</sup> have used a pseudo-random binary sequence as the transmitted signal. Cross correlating this incident signal with

the reflected signal will result in the impulse response function of the system. The deconvolution in their system is achieved by hardware implementation. As in other cases, the inherent bandwidth limitation of the transducer would deteriorate the resulting impulse response function and a processing technique similar to the ones described above will have to be used. Despite this drawback this method has the advantage of a high average to peak power ratio - almost equal to unity. This feature is very useful in increasing the range in in-vivo examinations, as there is a limit on the peak power that can be applied without any harmful effect.

In all the impediographic methods listed above, the attenuation due to the intervening material has been neglected. The accuracy of these methods therefore is limited by this factor. The method under investigation in this thesis not only takes into account the attenuation in determining the impedance, but also allows the determination of the attenuation itself.

Attenuation of ultrasound in biological tissue has been under investigation for some time. The early researchers concentrated on measuring the variation of the ultrasonic attenuation with frequency in different tissue types<sup>8</sup> and in understanding the mechanisms of ultrasonic attenuation<sup>7</sup>. Kuc, et al.<sup>18</sup> have outlined a method which uses a Gaussian pulse to measure the attenuation coefficient slope of soft tissue. Lizzi, et al.<sup>20</sup> have demonstrated a method which gives the attenuation characteristics of a homogeneous tissue as a function of frequency.

The use of ultrasonic attenuation for imaging purposes began very recently. Greanleaf, et al.<sup>9</sup> have developed a clinical

imaging system with transmissive ultrasonic tomography. In this system, ultrasonic pulses are transmitted through the breast in a coronal plane from many directions. The received signals are then processed for arrival times and the change in amplitude. These values are used in a convolution back projection reconstruction algorithm to obtain estimates of the two dimensional distribution of acoustic speed and attenuation within the scanned plane of the breast.

Klepper, et al.<sup>16</sup> have used a phase insensitive detection method to find the attenuation distribution. They also used the acoustic pulses transmitted through the sample from various directions to construct an image using attenuation.

## CHAPTER II

### THEORETICAL CONSIDERATIONS

This chapter outlines the theoretical background necessary for the proposed method of attenuation and impedance measurement. <sup>P</sup> In the first section, a layered structure is assumed. This model results in a straight forward determination of the attenuation and impedance variations. <sup>Q</sup> The second section considers an inhomogeneous model, where the acoustic impedance is a continuous function of the distance. Any discontinuities would have to be handled by a combination of the two models. Due to the narrow bandwidth of the ultrasonic transducer, the impulse response function of the medium cannot be found accurately. Two methods that can be used to improve the accuracy of determining the impulse response function are described next.

#### 2.1 REFLECTIONS FROM A LAYERED STRUCTURE

Although biological tissues are acoustically complex, it should not necessarily be thought of as an inhomogeneous slurry of cellular material<sup>1</sup>. <sup>VE 53</sup> The microstructure of a tissue in general suggests that it consists of a multilayered, nonplanar, laminated structure in both longitudinal and lateral extent. Lateral variation of the acoustic boundaries can occur. The extent of the lateral area covered by the ultrasonic beam can be reduced by focussing. Hence the model like the one shown in Figure 2.1 can be used to represent certain biological structures.

0	1	2	...	i	i+1	...	N-1	N
$Z_0$	$Z_1$	$Z_2$	...	$Z_i$	$Z_{i+1}$	...	$Z_{N-1}$	$Z_0$
$\alpha_0$	$\alpha_1$	$\alpha_2$	...	$\alpha_i$	$\alpha_{i+1}$	...	$\alpha_{N-1}$	$\alpha_0$
$\tau_0$	$\tau_1$	$\tau_2$	...	$\tau_i$	$\tau_{i+1}$	...	$\tau_{N-1}$	$\tau_0$
	$r_1$	$r_2$	$r_3$ ...	$r_i$	$r_{i+1}$	$r_{i+2}$ ...	$r_{N-1}$	$r_N$

FIGURE 2.1 A one dimensional layered structure

Consider an object which consists of  $N+1$  layers as shown in Figure 2.1. ~~The first~~ The first and the last layers are assumed to be made of the same material. The following notation is used.

$Z_i$  = acoustic impedance of the  $i$ th layer

$\alpha_i$  = attenuation coefficient of the  $i$ th layer in  $\text{Np/s}$

$\tau_i$  = time taken for the wave to propagate through the  $i$ th layer

$r_i$  = reflection coefficient at the boundary between  $(i-1)$ st and  $i$ th layers

Note that the attenuation coefficient is given in  $\text{Np/s}$ . This can be related to the attenuation in  $\text{Np/m}$  as

$$\alpha (\text{Np/s}) = \alpha (\text{Np/m}) \times c (\text{m/s}) \quad (2.1.1)$$

where  $c$  is the velocity of propagation of the ultrasonic wave.



The following assumptions are made.

1. Only (first) and (second order) reflections are considered. This can be justified for most biological structures, where the change of acoustic impedance from one layer to the next is not very large. If there is a large change in the impedance from one layer to the next, as is the case of a bone surrounded by soft tissue, multiple reflections may occur.
2. Each layer is homogeneous, i.e. there is no change in acoustical properties within each layer.
3. The width of boundaries between the layers is small compared to the acoustic wave length.

The response of the structure to an impulse can be derived as follows. The impulse response consists of N impulses; each corresponds to a reflection at one of the boundaries. Figure 2.2 shows the amplitude relationships at each boundary. The total impulse response due to various layers can be expressed as

$$h(t) = \sum_{i=1}^M a_i \delta(t-t_i) \quad (2.1.2)$$

where

$$t_i = \sum_{k=0}^{i-1} 2 \tau_k \quad (2.1.3)$$

$$a_i = \exp(-2\alpha_0 \tau_0) r_i \prod_{k=1}^{i-1} (1-r_k^2) \exp(-2\alpha_k \tau_k) \quad (2.1.4)$$

$$r_i = \frac{Z_i - Z_{i-1}}{Z_i + Z_{i-1}} \quad (2.1.5)$$

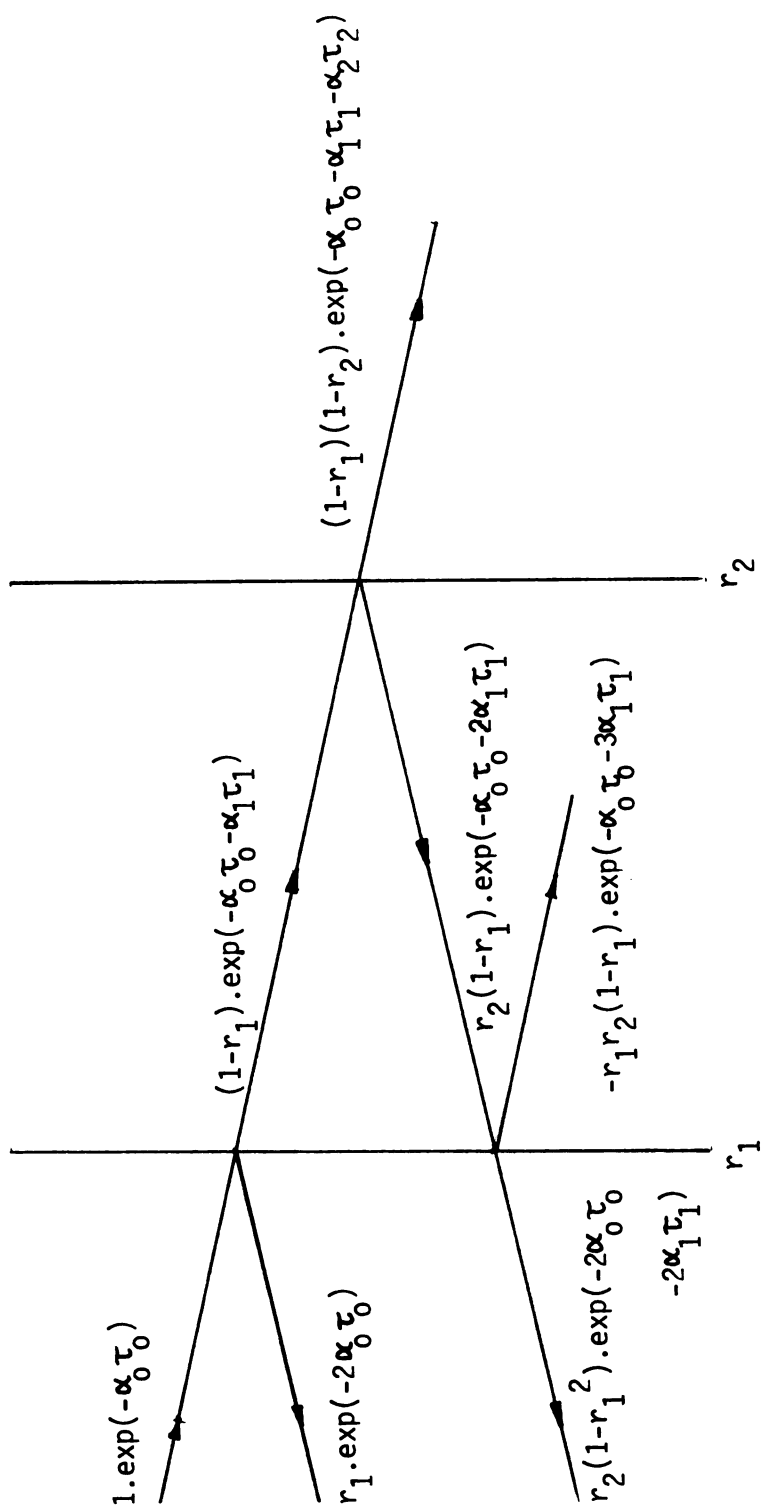


FIGURE 2.2 First and second order reflections from a layered structure

## 2.2 REFLECTIONS FROM AN ARBITRARY IMPEDANCE PROFILE

In this section the results of section 2.1 are extended for a structure with continuous variation of impedance.<sup>\*</sup> The inhomogeneous medium can be assumed to consist of a large number of parallel homogeneous layers with very small thickness as shown in Figure 2.3.

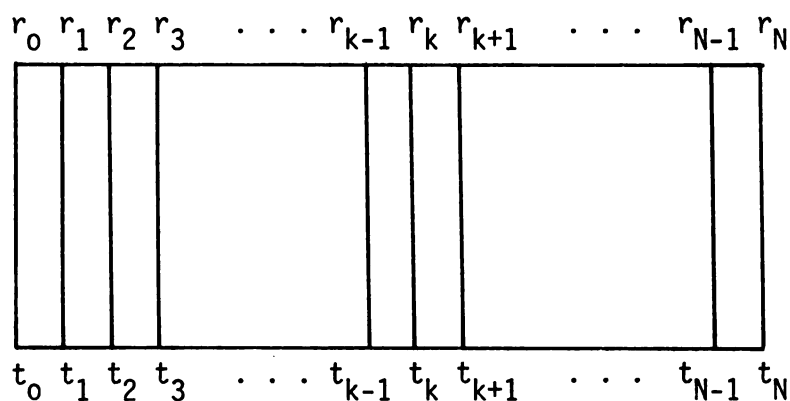


FIGURE 2.3 A one dimensional inhomogeneous structure

The impulse response function of the structure shown in Figure 2.3 can be written using equation (2.1.2)-(2.1.5) as

$$h(t) = \sum_{i=0}^N a_i \delta(t-t_i) \quad (2.2.1)$$

For the  $k$ th and  $(k-1)$ st layers,

$$h(t_k) = a_k \quad (2.2.2)$$

$$h(t_{k-1}) = a_{k-1} \quad (2.2.3)$$

Therefore,

$$\frac{h(t_k)}{h(t_{k-1})} = \frac{a_k}{a_{k-1}} \quad (2.2.4)$$

Substituting for  $a_k$  and  $a_{k-1}$  from equation (2.1.4),

$$\begin{aligned} \frac{h(t_k)}{h(t_{k-1})} &= \frac{r_k \prod_{j=1}^{k-1} (1-r_j^2) \exp(-2\alpha_j \tau_j)}{r_{k-1} \prod_{j=1}^{k-2} (1-r_j^2) \exp(-2\alpha_j \tau_j)} \\ &= \frac{r_k (1-r_{k-1}^2) \exp(-2\alpha_{k-1} \tau_{k-1})}{r_{k-1}} \end{aligned} \quad (2.2.5)$$

But from equation (2.1.3),

$$2\tau_{k-1} = t_k - t_{k-1} \quad (2.2.6)$$

Hence the ratio of the amplitudes of the impulse response function at  $t = t_k$  and  $t = t_{k-1}$  becomes

$$\frac{h(t_k)}{h(t_{k-1})} = \frac{r_k (1-r_{k-1}^2) \exp(-\alpha_{k-1} (t_k - t_{k-1}))}{r_{k-1}}$$

which can be expressed as

$$\begin{aligned} \ln h(t_k) - \ln h(t_{k-1}) &= \ln r_k - \ln r_{k-1} + \ln(1-r_{k-1}^2) \\ &\quad + \ln(\exp(-\alpha_{k-1} (t_k - t_{k-1}))) \end{aligned} \quad (2.2.7)$$

From equation (2.1.5), the ratio of acoustic impedances of the two layers is given by,

$$\frac{1 + r_k}{1 - r_k} = \frac{Z_k}{Z_{k-1}}$$

Hence,

$$\begin{aligned} \ln Z_k - \ln Z_{k-1} &= \ln(1+r_k) - \ln(1-r_k) \\ \lim_{r_k \rightarrow 0} \ln Z_k - \ln Z_{k-1} &= 2 r_k \end{aligned} \quad (2.2.8)$$

Also,

$$\lim_{r_k \rightarrow 0} \ln(1-r_k^2) = -r_k^2 \quad (2.2.9)$$

From equations (2.2.7) - (2.2.9),

$$\begin{aligned} \ln h(t_k) - \ln h(t_{k-1}) &= \ln\left(\frac{1}{2}(\ln Z_k - \ln Z_{k-1})\right) \\ &\quad - \ln\left(\frac{1}{2}(\ln Z_{k-1} - \ln Z_{k-2})\right) \\ &\quad + \frac{1}{4}(\ln Z_{k-1} - \ln Z_{k-2})^2 \\ &\quad + \ln(\exp(-\alpha_{k-1}(t_k - t_{k-1}))) \\ &= \ln(\ln Z_k - \ln Z_{k-1}) \\ &\quad - \ln(\ln Z_{k-1} - \ln Z_{k-2}) \\ &\quad + \frac{1}{4}(\ln Z_k - \ln Z_{k-1})^2 \\ &\quad + \ln(\exp(-\alpha_{k-1}(t_k - t_{k-1}))) \end{aligned}$$

$$\text{Let } t_k - t_{k-1} = \Delta t$$

$$\begin{aligned}
\frac{\ln h(t_k) - \ln h(t_k - \Delta t)}{\Delta t} \cdot \Delta t &= \ln \frac{\ln Z_k - \ln Z_{k-1}}{\Delta t} \\
&- \ln \frac{\ln Z_{k-1} - \ln Z_{k-2}}{\Delta t} \\
&+ \frac{1}{4}(\Delta t)^2 \left[ \frac{\ln Z_k - \ln Z_{k-1}}{\Delta t} \right]^2 \\
&+ \ln(\exp(-\alpha_{k-1}(t_k - t_{k-1})))
\end{aligned}$$

For an inhomogeneous medium,

$$t_k - t_{k-1} = \Delta t \rightarrow 0$$

Hence as  $\lim_{\Delta t \rightarrow 0}$ ,

$$\begin{aligned}
\frac{d}{dt} \ln h(t) \Big|_{t=t_k} \cdot \Delta t &= \ln \frac{d}{dt} \ln Z \Big|_{t=t_k} - \ln \frac{d}{dt} \ln Z \Big|_{t=t_{k-1}} \\
&+ \frac{\Delta t^2}{4} \left[ \frac{d}{dt} \ln Z \Big|_{t=t_k} \right]^2 \\
&+ \ln(\exp(-\alpha_{k-1} t_k)) \\
&- \ln(\exp(-\alpha_{k-1} t_{k-1})) \quad (2.2.10)
\end{aligned}$$

Adding and subtracting  $\ln(\exp(-\alpha_{k-2} t_{k-1}))$  from the right side of equation (2.2.10),

$$\begin{aligned}
\frac{d}{dt} \ln h(t) \Big|_{t=t_k} \cdot \Delta t &= \ln(\exp(-\alpha_{k-1} t_k \cdot \frac{d}{dt} \ln Z \Big|_{t=t_k})) \\
&- \ln(\exp(-\alpha_{k-2} t_{k-1} \cdot \frac{d}{dt} \ln Z \Big|_{t=t_{k-1}})) \\
&- \ln(\exp(-(\alpha_{k-1} - \alpha_{k-2}) t_{k-1})) \\
&+ \frac{\Delta t^2}{4} \left[ \frac{d}{dt} \ln Z \Big|_{t=t_k} \right]^2 \quad (2.2.11)
\end{aligned}$$

Using the identity,

$$\text{Ln}(\exp x) = x$$

and letting

$$\alpha_{k-1} - \alpha_{k-2} = \Delta \alpha,$$

$$\begin{aligned} \left. \frac{d}{dt} \text{Ln } h(t) \right|_{t=t_k} &= \frac{1}{\Delta t} \left[ \text{Ln}(\exp(-\alpha_{k-1} t_k \cdot \frac{d}{dt} \text{Ln } Z \Big|_{t=t_k})) \right. \\ &\quad \left. - \text{Ln}(\exp(-\alpha_{k-2} t_{k-1} \cdot \frac{d}{dt} \text{Ln } Z \Big|_{t=t_{k-1}})) \right] \\ &\quad + \frac{\Delta \alpha}{\Delta t} t_{k-1} + \frac{\Delta t}{4} \left[ \frac{d}{dt} \text{Ln } Z \Big|_{t=t_k} \right]^2 \end{aligned}$$

As  $\lim_{\Delta t \rightarrow 0}$ ,

$$\frac{d}{dt} \text{Ln } h(t) = \frac{d}{dt} \text{Ln} \left[ \exp(-\alpha t) \cdot \frac{d}{dt} \text{Ln } Z \right] + \frac{d\alpha}{dt} \cdot t \quad (2.2.12)$$

Note that  $\alpha$  is a function of  $t$ .

Integrating equation (2.2.12) with respect to  $t$  yields

$$\begin{aligned} \text{Ln } h(t) &= \text{Ln} \left[ \exp(-\alpha t) \cdot \frac{d}{dt} \text{Ln } Z \right] + \int t \cdot \frac{d\alpha}{dt} \cdot dt + c \\ &= -\alpha t + \text{Ln} \left[ \frac{d}{dt} \text{Ln } Z \right] + \alpha t - \int \alpha \cdot dt + c \\ &= \text{Ln} \frac{d}{dt} \text{Ln } Z + \text{Ln} \exp(-\int \alpha \cdot dt) + c \\ &= \text{Ln} \left[ C \frac{d}{dt} \text{Ln } Z \cdot \exp(-\int \alpha \cdot dt) \right] \end{aligned}$$

where  $C$  is the integration constant.

The impulse response function is thus given by

$$\underline{h(t) = C \frac{d}{dt} \text{Ln } Z \cdot \exp(-\int \alpha \cdot dt)} \quad (2.2.13)$$

The coefficient  $C$  can be determined by considering a lossless

medium, i.e. a medium with  $\alpha=0$ , The relationship between  $h(t)$  and

Z for such a medium is given by<sup>13</sup>,

$$h(t) = \frac{1}{2} \frac{d}{dt} \ln Z \quad (2.2.14)$$

Therefore,

$$C = \frac{1}{2} \quad (2.2.15)$$

The complete impulse response is thus given by,

$$h(t) = \frac{1}{2} \exp\left(-\int_0^t \alpha(t) \cdot dt\right) \frac{d}{dt} \ln Z(t) \quad (2.2.16)$$

where

\*  $Z(t)$  = ~~impedance encountered by the ultrasonic pulse at~~  
time t.

\*  $\alpha(t)$  = ~~attenuation coefficient (Np/s) encountered by the~~  
ultrasonic pulse at time t.

### 2.3 IMPROVEMENT OF THE ACCURACY OF THE IMPULSE RESPONSE FUNCTION

The acoustic impulse response function of an object can be obtained by deconvolving the incident and the reflected signals. It has been shown that a narrow band source is necessary to maintain a good lateral resolution<sup>2</sup>. Practically, even in cases where lateral resolution is not of main concern, the incident spectrum is limited by the transducer bandwidth. The conventional approach for determination of the impulse response function consists of the following steps.

1. Obtain the Fourier transforms  $X(f)$  and  $Y(f)$  of the incident and reflected signals  $x(t)$  and  $y(t)$  respectively.
2. The transfer function  $H(f)$  is given by

$$H(f) = \frac{Y(f)}{X(f)} \quad (2.3.1)$$



3. The impulse response function  $h(t)$  is obtained by determining the inverse Fourier transform of  $H(f) \cdot W(f)$ , where  $W(f)$  is a window function in the frequency domain, which attenuates rapidly outside the frequency band of  $X(f)$ .

$$h(t) = F^{-1}(H(f) \cdot W(f)) \quad (2.3.2)$$

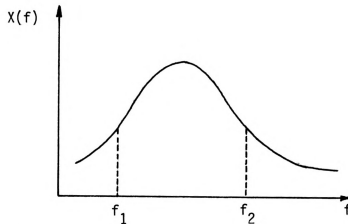


FIGURE 2.4 Frequency spectrum of a typical incident wave

The frequency spectrum of a typical incident waveform is shown in Figure 2.4. Due to the presense of noise, the transfer function computed using equation (2.3.1) is not reliable at the fringes of the spectrum  $X(f)$ , outside the frequency band  $(f_1, f_2)$ . In the time domain this will result in an ambiguity in the location and amplitude of the returned echoes, due to noise and interference from overlapping echoes. This ambiguity can be reduced by restoring the frequency components of the impulse response function  $h(t)$ , that are outside the significant frequency band of the incident spectrum. Two techniques that can be used for this purpose are described below.

### 2.3.1 FREQUENCY RESTORED IMPULSE RESPONSE FUNCTION<sup>23</sup>

This method is suitable for improvement of the impulse response function of a layered structure. Due to the presense of noise, the calculated transfer function will have a value  $H_0(f)$ , which is unreliable outside the main frequency band  $(f_1, f_2)$ . The resulting error can be reduced by multiplying  $H_0(f)$  by a suitable window function  $W(f)$  that attenuates rapidly outside this band.

$$H_w(f) = H_0(f).W(f) \quad (2.3.3)$$

where

$$H_0(f) = \frac{Y(f)}{X(f)} \quad (2.3.4)$$

The inverse Fourier transform of  $H_w(f)$ ,  $h_w(t)$ , is a modulated waveform and the locations  $t_i$  and the amplitudes  $a_i$ ,  $i=1,2,\dots k$  of its peaks determined by a demodulation scheme give a first order estimate of the interface locations and the corresponding reflection coefficients. This estimate can be improved by the following procedure.

1. Form the frequency spectrum

$$P(f) = \sum_i a_i \exp(-j2\pi f t_i) \quad (2.3.5)$$

2. Form the new estimation of the transfer function

$$H_1(f) = H_0(f).W(f) + (1 - W(f)).P(f) \quad (2.3.6)$$

3. The inverse Fourier transform  $h_1(t)$  of  $H_1(f)$  is the new estimate of the impulse response function.

$$h_1(t) = F^{-1}(H_1(f)) \quad (2.3.7)$$

4. Detect the peak amplitudes  $a_i$  and their positions  $t_i$  and repeat steps 1-4. After two or three iterations, a considerable improvement can be expected.

### 2.3.2 IMPROVEMENT OF THE IMPULSE RESPONSE FUNCTION BY SPECTRAL EXTRAPOLATION<sup>22</sup>

This method extrapolates the frequency components of  $H(f)$  outside the reliable frequency band  $(f_1, f_2)$  by using the frequency components inside the reliable band. This technique is applicable for impulse response functions of both layered and homogeneous structures. The reflected signal has a finite time duration which depends on the thickness of the object under test. This fact is made use of in order to extrapolate the spectrum. The procedure is as follows.

1. Calculate the transfer function  $H(f)$  using equation (2.3.1.).

(See Figure 2.5a)

2. Let

$$W_1(f) = \begin{cases} H(f) & f_1 < |f| < f_2 \\ 0 & \text{otherwise} \end{cases} \quad (2.3.8)$$

(See Figure 2.5b)

3. Inverse Fourier transform  $W_1(f)$  to obtain  $w_1(t)$

$$w_1(t) = F^{-1} W_1(f) \quad (2.3.9)$$

(See Figure 2.5c)

4. The duration of the impulse response is assumed to be  $T$ .  $T$  depends on the thickness of the object. The new estimate of the impulse response function is

$$h_1(t) = \begin{cases} w_1(t) & 0 < t < T \\ 0 & \text{otherwise} \end{cases} \quad (2.3.10)$$

(See Figure 2.5d)

5. Compute the Fourier transform  $H_1(f)$  of  $h_1(t)$  and form the spectrum

$$W_2(f) = \begin{cases} H(f) = W_1(f) & f_1 < |f| < f_2 \\ H_1(f) & \text{otherwise} \end{cases} \quad (2.3.11)$$

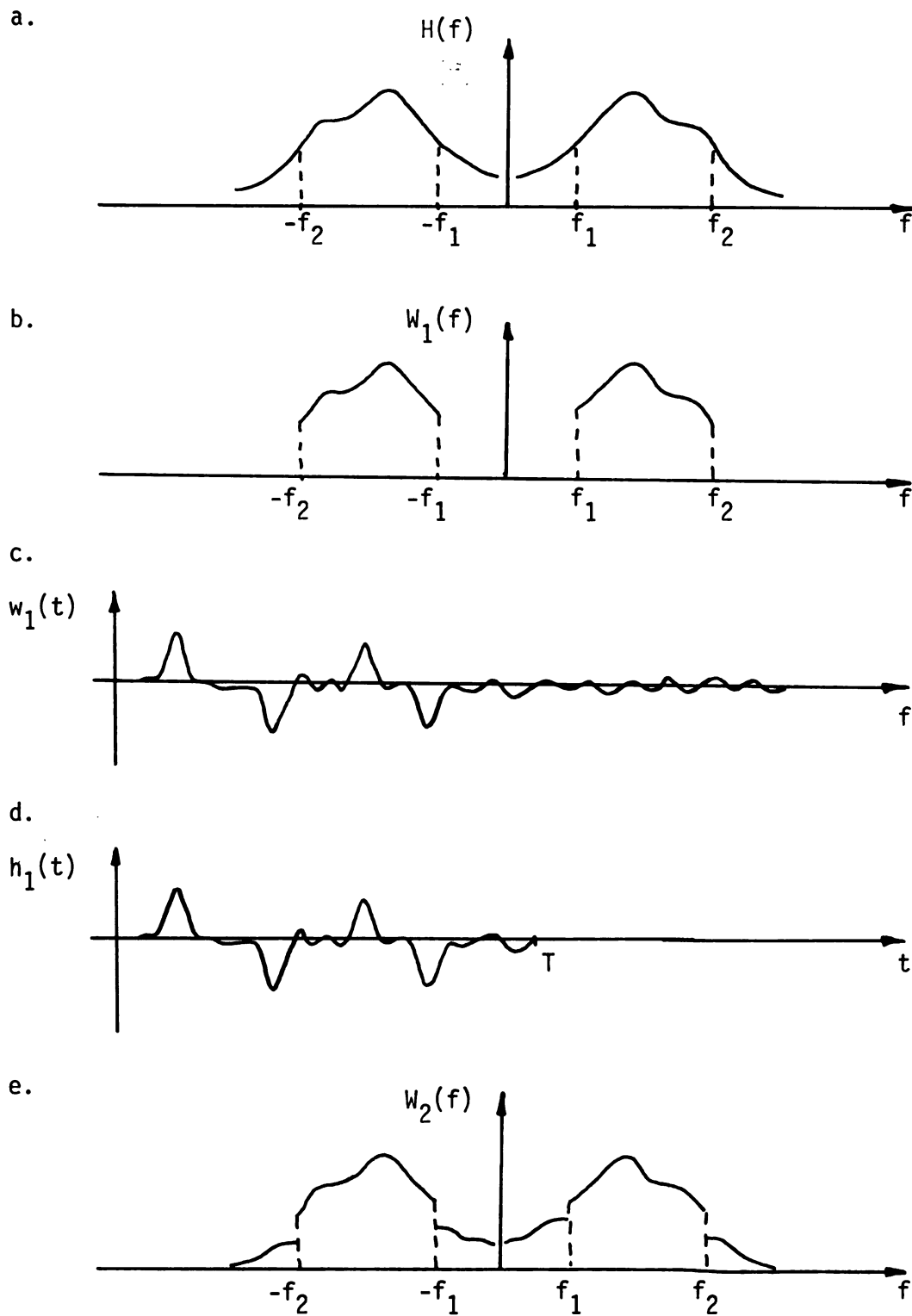


FIGURE 2.5 Spectral extrapolation for impulse response function improvement.

$W_2(f)$  is shown in Figure 2.5e.

6. Repeat steps 3,4,5 until the required improvement is achieved.

Next chapter makes use of the theory developed in sections 2.1 and 2.2 to devise a method to find the variation of attenuation along the path of propagation of an ultrasound signal.

## ATTENUATION VARIATION FROM REFLECTED SIGNALS

This chapter explains how the information about the variation of attenuation inside an object can be obtained by using the incident and reflected signals. As two reflected signals, obtained by transmitting a wave from either side of the object (see Figure 3.1) are required, this method is applicable only for objects with a short length along the beam axis. However, the range can be increased by increasing the amount of incident signal power.

The first section assumes the object to be a layered structure. An inhomogeneous object, where the acoustical impedance is a continuous function of the distance is considered next. The impulse response of the object when interrogated from the opposite sides are given by  $h_1(t)$  and  $h_2(t)$ .

### 3.1 RELATIONSHIP OF ATTENUATION TO IMPULSE RESPONSE FUNCTION OF A LAYERED OBJECT

Consider a layered structure with  $N+1$  layers -  $N$  interfaces - as shown in Figure 3.2. The first and last layers are assumed to be the same material, which normally is the case because the object is immersed in water. Using the results of section 2.1,  $h_1(t)$  and  $h_2(t)$  can be written as

$$h_1(t) = \sum_{i=1}^N a_i \delta(t-t_i) \quad (3.1.1)$$

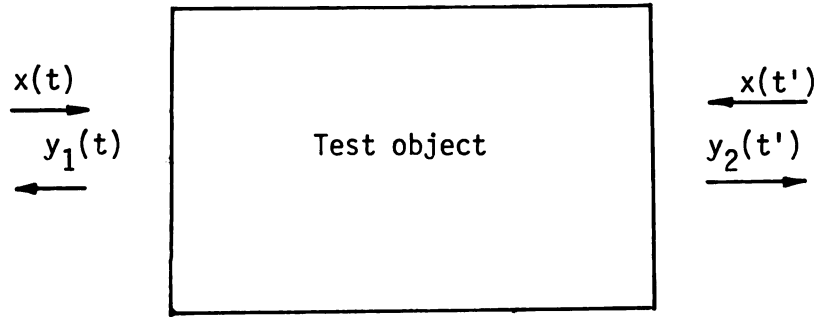


FIGURE 3.1 Bi-directional ultrasonic interrogation.

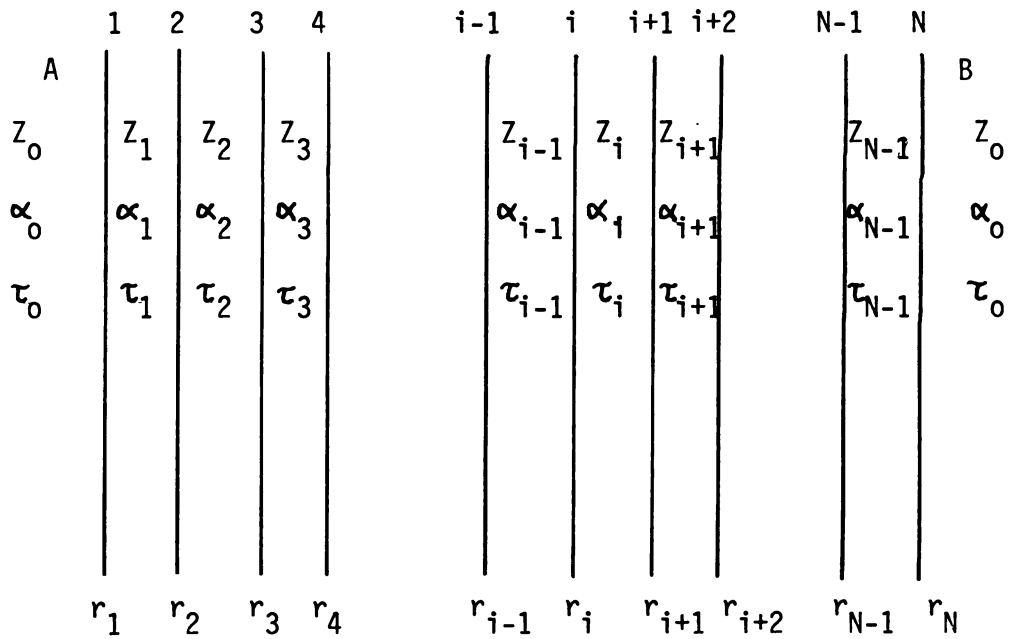


FIGURE 3.2 A layered structure.

where,

$$t_i = \sum_{k=0}^i 2\tau_k \quad (3.1.2)$$

$$a_i = \exp(-2\alpha_0 \tau_0) \cdot r_i \prod_{k=1}^{i-1} (1-r_k^2) \exp(-2\alpha_k \tau_k) \quad (3.1.3)$$

$$r_i = \frac{Z_i - Z_{i-1}}{Z_i + Z_{i-1}} \quad (3.1.4)$$

Similarly,

$$h_2(t) = \sum_{j=1}^N b_j \delta(t-t'_j) \quad (3.1.5)$$

where,

$$t'_j = \sum_{k=j}^N 2\tau_k \quad (3.1.6)$$

$$b_j = - \exp(-2\alpha_j \tau_j) \cdot r_j \prod_{k=j+1}^N (1-r_k^2) \exp(-2\alpha_k \tau_k) \quad (3.1.7)$$

The minus sign accounts for the fact that the reflection coefficient changes its sign when the incident wave is from the opposite side.

The values  $a_i$  and  $b_j$  ( $i, j = 1, 2, \dots, N$ ) can be read directly from the impulse response functions  $h_1(t)$  and  $h_2(t)$ .

Using equation (3.1.3), the ratio of  $a_i$  to  $a_{i+1}$  is

$$\begin{aligned} \frac{a_i}{a_{i+1}} &= \frac{\exp(-2\alpha_0 \tau_0) \cdot r_i \prod_{k=1}^{i-1} (1-r_k^2) \exp(-2\alpha_k \tau_k)}{\exp(-2\alpha_0 \tau_0) \cdot r_{i+1} \prod_{k=1}^i (1-r_k^2) \exp(-2\alpha_k \tau_k)} \\ &= \frac{r_i}{r_{i+1} (1-r_i^2) \exp(-2\alpha_i \tau_i)} \end{aligned} \quad (3.1.8)$$



Similarly, from equation (3.1.7)

$$\begin{aligned} \frac{b_i}{b_{i+1}} &= \frac{\exp(-2\alpha_i \tau_i) \cdot r_i \prod_{k=i+1}^N (1-r_k^2) \exp(-2\alpha_k \tau_k)}{\exp(-2\alpha_{i+1} \tau_{i+1}) \cdot r_{i+1} \prod_{k=i+2}^N (1-r_k^2) \exp(-2\alpha_k \tau_k)} \\ &= \frac{\exp(-2\alpha_i \tau_i) \cdot r_i (1-r_{i+1}^2)}{r_{i+1}} \end{aligned} \quad (3.1.9)$$

Using equations (3.1.8) and (3.1.9),

$$\frac{a_i b_i}{a_{i+1} b_{i+1}} = \frac{r_i^2 (1-r_{i+1}^2)}{(1-r_i^2) r_{i+1}^2} \quad (3.1.10)$$

Define  $R_i$  as

$$\star \underline{R_i} = \frac{r_i^2}{1-r_i^2} \Rightarrow \quad (3.1.11)$$

Then

$$\frac{a_i b_i}{a_{i+1} b_{i+1}} = \frac{R_i}{R_{i+1}}$$

or

$$R_{i+1} = R_i \cdot \left[ \frac{a_{i+1} b_{i+1}}{a_i b_i} \right] \quad (3.1.12)$$

$$r_{i+1} = S_{i+1} \left[ \frac{R_{i+1}}{R_{i+1} + 1} \right]^{\frac{1}{2}} \quad (3.1.13)$$

where

$$S_i = \begin{cases} +1 & a_{i+1} > 0 \\ -1 & a_{i+1} < 0 \end{cases} \quad (3.1.14)$$

Dividing equation (3.1.8) by equation (3.1.9),

$$\frac{a_i b_{i+1}}{a_{i+1} b_i} = \frac{r_i}{r_{i+1} (1-r_i^2) \exp(-2\alpha_i \tau_i)} \cdot \frac{r_{i+1}}{r_i (1-r_{i+1}^2) \exp(-2\alpha_i \tau_i)}$$

which can be written as,

$$\exp(4\alpha_i \tau_i) = \frac{a_i b_{i+1}}{a_{i+1} b_i} \cdot (1-r_i^2) (1-r_{i+1}^2)$$

Hence the attenuation constant is given by,

$$\alpha_i = \frac{1}{4\tau_i} \cdot \ln \left[ \frac{a_i b_{i+1}}{a_{i+1} b_i} \cdot (1-r_i^2) (1-r_{i+1}^2) \right] \quad (3.1.15)$$

The following algorithm can be used to find the reflection coefficient at each interface and the attenuation and impedance in each layer. The value of  $\alpha_0$  is assumed to be known.

1. From equations (3.1.3) and (3.1.7)

$$r_1 = \exp(2\alpha_0 \tau_0) a_1 \quad (3.1.16)$$

$$r_N = -\exp(2\alpha_0 \tau_0) b_N \quad (3.1.17)$$

$a_1, b_N$  and  $\tau_0$  can be read from impulse response functions.

2. Use equations (3.1.11) through (3.1.14) with  $i=1$  to find  $R_i$ ,  $R_{i+1}$  and  $r_{i+1}$  respectively.

$$R_i = \frac{r_i^2}{1 - r_i^2} \quad (3.1.11)$$

$$R_{i+1} = R_i \cdot \left[ \frac{a_{i+1} b_{i+1}}{a_i b_i} \right] \quad (3.1.12)$$

$$r_{i+1} = S_{i+1} \left[ \frac{R_{i+1}}{R_{i+1} + 1} \right]^{\frac{1}{2}} \quad (3.1.13)$$

where,

$$S_{i+1} = \begin{cases} +1 & \text{if } a_{i+1} > 0 \\ -1 & \text{if } a_{i+1} < 0 \end{cases} \quad (3.1.14)$$

3. Use equation (3.1.15) to find the attenuation constant  $\alpha_i$ ,

$$\alpha_i = \frac{1}{4\tau_i} \cdot \ln \left[ \frac{a_i b_{i+1}}{a_{i+1} b_i} \cdot (1-r_i^2) (1-r_{i+1}^2) \right] \quad (3.1.15)$$

4. From equation (3.1.4),

$$\frac{Z_i}{Z_0} = \frac{1 + r_i}{1 - r_i} \cdot \frac{Z_{i-1}}{Z_0} \quad (3.1.18)$$

This equation can be used to find the normalized impedance of the i th layer.

5. Repeat steps 2,3 and 4 until all the impedances, attenuation coefficients and reflection coefficients are found.

### 3.2 RELATIONSHIP OF ATTENUATION TO IMPULSE RESPONSE FUNCTION OF AN INHOMOGENEOUS MEDIUM

In this case, the medium is assumed to have a continuous variation of impedance along the path of propagation as shown in Figure 3.3.

The following notation is used.

$x(t)$  = incident waveform

$y_1(t)$  = reflected waveform when the object is  
interrogated from left

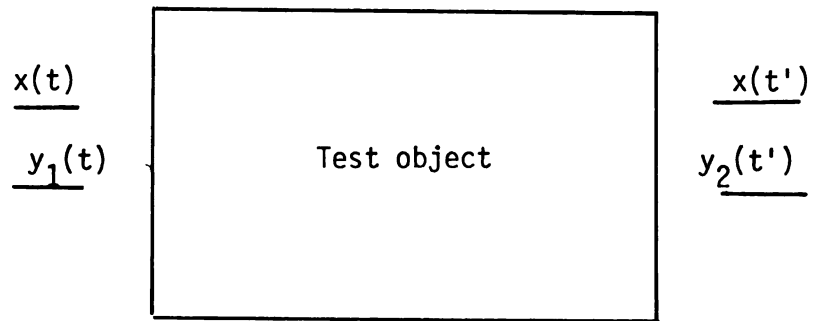


FIGURE 3.3 An inhomogeneous medium.

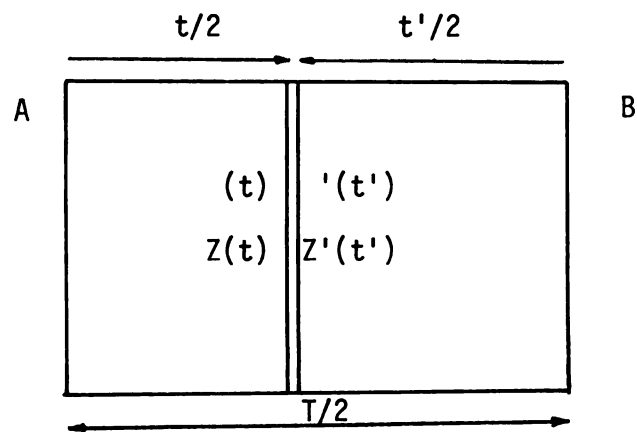


FIGURE 3.4 Time relationships for bi-directional ultrasonic interrogation.

- $y_2(t)$  = reflected waveform when the object is interrogated from right  
 $h_1(t)$  = impulse response function of the medium when interrogated from left,  
 i.e.  $y_1(t) = x(t) * h_1(t)$   
 $h_2(t)$  = impulse response function of the medium when interrogated from right,  
 i.e.  $y_2(t) = x(t) * h_2(t)$   
 $Z(t)$  = impedance encountered by the acoustic signal, when it has travelled a time  $t/2$  from the left end  
 $Z'(t')$  = impedance encountered by the acoustic signal, when it has travelled a time  $t'/2$  from the right end  
 $\alpha(t)$  = attenuation coefficient (Np/s) encountered by the acoustic signal, when it has travelled a time  $t/2$  from the left end  
 $\alpha'(t')$  = attenuation coefficient (Np/s) encountered by the acoustic signal, when it has travelled a time  $t'/2$  from the right end  
 $T$  = total round trip time of the ultrasound signal  
 - i.e. time taken for the signal to return after being reflected at the far end.

From Figure 3.4 it is seen that  $h_1(t)$  and  $h_2(t')$ , where  $t' = T - t$ , corresponds to reflections from the same layer in the medium.

Hence,

$$Z(t) = Z'(T-t) \quad (3.2.1)$$

$$\alpha(t) = \alpha'(T-t) \quad (3.2.2)$$

From equation (2.2.16),

$$h_1(t) = \frac{1}{2} \exp\left(-\int_0^t \alpha(t).dt\right) \cdot \frac{d}{dt} \ln Z(t) \quad (3.2.3)$$

$$h_2(t') = \frac{1}{2} \exp\left(-\int_0^{t'} \alpha'(t).dt\right) \cdot \frac{d}{dt'} \ln Z'(t') \quad (3.2.4)$$

Now, the aim is to find the attenuation and the impedance of a thin segment of the body as shown in Figure 3.4. From equation (3.2.3) with  $t=t_1$  and  $t=t_2$ ,

$$\begin{aligned} \frac{h_1(t_1)}{h_1(t_2)} &= \frac{\frac{1}{2} \exp\left(-\int_0^{t_1} \alpha(t).dt\right) \cdot \frac{d}{dt} \ln Z(t) \Big|_{t=t_1}}{\frac{1}{2} \exp\left(-\int_0^{t_2} \alpha(t).dt\right) \cdot \frac{d}{dt} \ln Z(t) \Big|_{t=t_2}} \\ &= \frac{\exp\left(-\int_{t_2}^{t_1} \alpha(t).dt\right) \cdot \frac{d}{dt} \ln Z(t) \Big|_{t=t_1}}{\frac{d}{dt} \ln Z(t) \Big|_{t=t_2}} \end{aligned} \quad (3.2.5)$$

Similarly,

$$\frac{h_2(t_2')}{h_2(t_1')} = \frac{\exp\left(-\int_{t_1'}^{t_2'} \alpha'(t).dt\right) \cdot \frac{d}{dt'} \ln Z'(t') \Big|_{t'=t_2'}}{\frac{d}{dt'} \ln Z'(t') \Big|_{t'=t_1'}} \quad (3.2.6)$$

Also

$$t_1 + t_1' = T \quad (3.2.7)$$

and

$$t_2 + t_2' = T \quad (3.2.8)$$

Using equations (3.2.1), (3.2.2), (3.2.7) and (3.2.8),

$$\left. \frac{d}{dt} \ln Z(t) \right|_{t=t_1} = \ominus \left. \frac{d}{dt'} \ln Z'(t') \right|_{t'=t'_1} \quad (3.2.9)$$

$$\left. \frac{d}{dt} \ln Z(t) \right|_{t=t_2} = \ominus \left. \frac{d}{dt'} \ln Z'(t') \right|_{t'=t'_2} \quad (3.2.10)$$

$$\int_{t_1}^{t_2} \alpha(t).dt = \int_{t'_2}^{t'_1} \alpha'(t).dt \quad (3.2.11)$$

Multiplying equations (3.2.5) and (3.2.6),

$$\begin{aligned} \frac{h_1(t_1) h_2(t'_2)}{h_1(t_2) h_2(t'_1)} &= \exp\left(-\int_{t_2}^{t_1} \alpha(t).dt\right) \cdot \exp\left(-\int_{t'_1}^{t'_2} \alpha'(t).dt\right) \\ &\cdot \frac{\left. \frac{d}{dt} \ln Z(t) \right|_{t=t_1}}{\left. \frac{d}{dt} \ln Z(t) \right|_{t=t_2}} \cdot \frac{\left. \frac{d}{dt'} \ln Z'(t') \right|_{t'=t'_2}}{\left. \frac{d}{dt'} \ln Z'(t') \right|_{t'=t'_1}} \end{aligned}$$

Using equations (3.2.9) and (3.2.10),

$$\frac{h_1(t_1) h_2(t'_2)}{h_1(t_2) h_2(t'_1)} = \exp\left(-2 \int_{t_2}^{t_1} \alpha(t).dt\right)$$

i.e. ,

$$\int_{t_2}^{t_1} \alpha(t).dt = \frac{1}{2} \ln \frac{h_1(t_2) h_2(t'_1)}{h_1(t_1) h_2(t'_2)} \quad (3.2.12)$$

From equations (3.2.3) and (3.2.4),

$$\begin{aligned} h_1(t_1) h_2(t'_1) &= \frac{1}{4} \exp\left(-\int_0^{t_1} \alpha(t).dt\right) \cdot \exp\left(-\int_0^{t'_1} \alpha'(t).dt\right) \\ &\cdot \left. \frac{d}{dt} \ln Z(t) \right|_{t=t_1} \cdot \left. \frac{d}{dt'} \ln Z'(t') \right|_{t'=t'_1} \end{aligned}$$

Using equations (3.2.1) and (3.2.9),

$$\begin{aligned}
 h_1(t_1) h_2(t_1') &= \frac{1}{4} \exp\left(-\int_0^{t_1} \alpha(t).dt\right) \cdot \exp\left(-\int_{t_1}^T \alpha(t).dt\right) \\
 &\quad \cdot (-1) \frac{d}{dt} \ln Z(t) \Big|_{t=t_1}^2 \\
 &= -\frac{1}{4} \exp\left(-\int_0^T \alpha(t).dt\right) \cdot \frac{d}{dt} \ln Z(t) \Big|_{t=t_1}^2
 \end{aligned}$$

This reduces to

$$\frac{d}{dt} \ln Z(t) = \exp\left(\frac{1}{2} \cdot \int_0^T \alpha(t).dt\right) \cdot \left[-4 h_1(t).h_2(T-t)\right]^{\frac{1}{2}}$$

By integrating with respect to time,

$$\begin{aligned}
 \ln \frac{Z(t)}{Z(0)} &= \left[ \exp\left(-\int_0^T \alpha(t).dt\right) \right]^{-\frac{1}{2}} \\
 &\quad \cdot \int_0^t \left[-4 h_1(t).h_2(T-t)\right]^{\frac{1}{2}} .dt
 \end{aligned} \tag{3.2.13}$$

Let

$$\star A_T = \exp\left(-\int_0^T \alpha(t).dt\right) \tag{3.2.14}$$

where  $A_T$  is the total attenuation of the medium,

From equations (3.2.13) and (3.2.14),

$$\ln \frac{Z(t)}{Z(0)} = (A_T)^{-\frac{1}{2}} \int_0^t \left[-4 h_1(t).h_2(T-t)\right]^{\frac{1}{2}} .dt \tag{3.2.15}$$

Equation (3.2.12) can be used to find the attenuation variation along the medium. The result can be used to determine  $A_T$  from equation (3.2.14). Finally, equation (3.2.15) can be used to find the variation of impedance along the path of propagation.



## CHAPTER IV

### EXPERIMENTAL PROCEDURE AND RESULTS

The theoretical development in section 3.1 was verified using two models. Section 4.1 outlines the procedure used to obtain the data -the incident and reflected wave forms. The method of analysing the data is given in section 4.2. Next, the results obtained for the two models are compared with the values obtained by direct measurements.

#### 4.1 DATA COLLECTION

The systems used for sample recording of incident and reflected signals are shown in Figures 4.1 and 4.2. To calculate the attenuation and impedance variation in the test object, the incident signal waveform and the reflected signal waveforms, when the ultrasound signal is applied on either side of the object, are required. The waveforms were manually sampled using the delayed sweep feature of the Tektronix 465 Cathode Ray Oscilloscope. A sampling rate of 10MHz was chosen, as the significant frequency components of the incident signal were below 5 MHz. The experimental procedure is as follows.

##### 1. Record the incident signal waveform.

This was done by observing the reflections at the air - water interface as shown in Figure 4.1. As the acoustic impedance of water is about 3700 times that of air<sup>25</sup>, total reflection with a phase change of 180° was assumed. The attenuation of ultrasound signal in water was neglected.

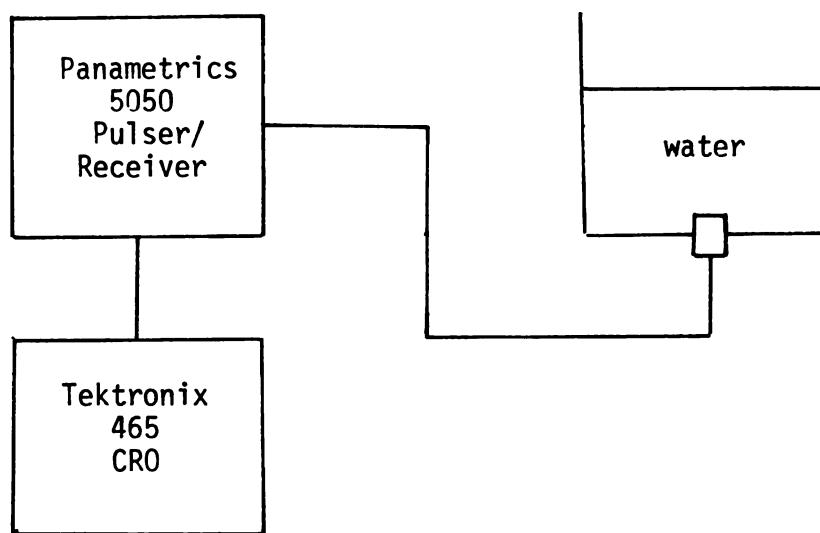


FIGURE 4.1 Incident waveform recording

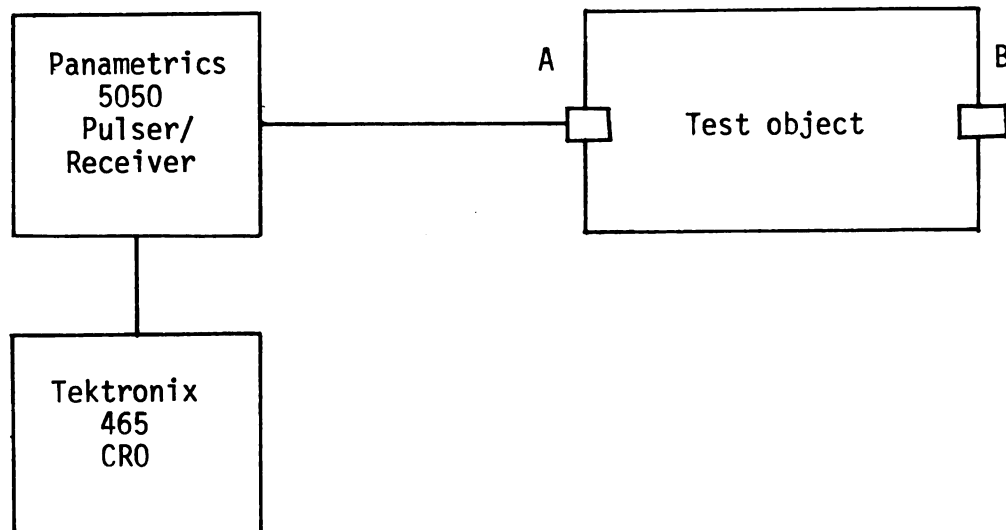


Figure 4.2 Reflected waveform recording

2. Record the reflected signal when interrogated from side A of the object.

This was done using the system shown in Figure 4.2.

3. Record the reflected signal when interrogated from side B of the object.

Same method as in 2 above.

#### 4.2 DATA PROCESSING

The following procedure was used to obtain the impedance and the attenuation variation of the object.

1. Estimate the acoustic impulse response function of the object when it is interrogated from either side of the object.

This was done using the following two methods.

##### a. Direct Impulse Response Function

The reflection function of the object,  $H(f)$  is the ratio of the Discrete Fourier Transforms of the reflected and incident signals.

$$H(f) = \frac{Y(f)}{X(f)} \quad (4.2.1)$$

As the spectrum of  $H(f)$  is unreliable outside the significant frequency band of  $X(f)$ , a Hanning filter  $W(f)$  was used to filter out the unreliable frequency components of  $H(f)$ .

$$\underline{H'(f)} = \frac{W(f) Y(f)}{X(f)} \quad (4.2.2)$$

where

$$W(f) = \begin{cases} \cos^2 \frac{\pi(f-f_0)}{2\Delta f} & f_0 - \Delta f < f < f_0 + \Delta f \\ 0 & \text{otherwise} \end{cases} \quad (4.2.3)$$

$f_0 - \Delta f < f < f_0 + \Delta f$  is the reliable frequency band of  $X(f)$ . The

inverse transform  $h'(t)$  of  $H'(f)$  is a filtered version of the impulse response function. The algorithm used for this method is given in Appendix A. The impulse response function is estimated using a software implemented amplitude detection scheme (Appendix C).

b. Frequency Restored Impulse Response Function

Section 2.3.1 outlines a method by which the impulse response function can be improved by estimating the frequency components outside the significant frequency band of the incident waveform. This method was used to find an improved impulse response function. The method of implementation is given in Appendix B. Amplitude detection scheme given in Appendix C was then used to find the echo amplitudes.

2. Obtain the variation of impedance and attenuation using the impulse response functions. This is done by using equations (3.1.11) through (3.1.17). Assuming the attenuation of ultrasound in water to be negligible, equations (3.1.11) through (3.1.17) can be written as follows.

$$r_1 = a_1 \quad (4.2.4)$$

$$r_N = -b_N \quad (4.2.5)$$

For  $i = 1, 2, \dots, N$ ,

$$R_i = \frac{r_i^2}{1 - r_i^2} \quad (4.2.6)$$

$$R_{i+1} = R_i \frac{a_{i+1} b_{i+1}}{a_i b_i} \quad (4.2.7)$$

$$r_{i+1} = S_{i+1} \left[ \frac{R_{i+1}}{1 + R_{i+1}} \right]^{\frac{1}{2}} \quad (4.2.8)$$

where

$$S_{i+1} = \begin{cases} +1 & \text{if } a_{i+1} > 0 \\ -1 & \text{if } a_{i+1} < 0 \end{cases} \quad (4.2.9)$$

$$\exp(-2\alpha_i \tau_i) = \left[ \frac{a_i b_{i+1}}{a_{i+1} b_i} \cdot (1 - r_i^2) \cdot (1 - r_{i+1}^2) \right]^{-\frac{1}{2}} \quad (4.2.10)$$

$$\alpha_i = \frac{1}{4\tau_i} \ln \left[ \frac{a_i b_{i+1}}{a_{i+1} b_i} \cdot (1 - r_i^2)(1 - r_{i+1}^2) \right] \quad (4.2.11)$$

and

$$\frac{Z_i}{Z_0} = \frac{1 + r_i}{1 - r_i} \cdot \frac{Z_{i-1}}{Z_0} \quad (4.2.12)$$

The following notation is used (See Figure 4.3)

- N = number of interfaces
- $r_i$  = reflection coefficient at the  $i$  th interface
- $a_i$  = magnitude of the reflected impulse due to the  $i$  th interface, when interrogated from side A
- $b_i$  = magnitude of the reflected impulse due to the  $i$  th interface, when interrogated from side B
- $\alpha_i$  = attenuation coefficient (Np/s) in the layer bounded by  $i$  th and  $i+1$  st interfaces
- $\tau_i$  = propagation time in the layer between  $i$  th and  $i+1$  st interfaces
- $Z_i$  = acoustic impedance of the layer between  $i$  th and  $i+1$  st interfaces

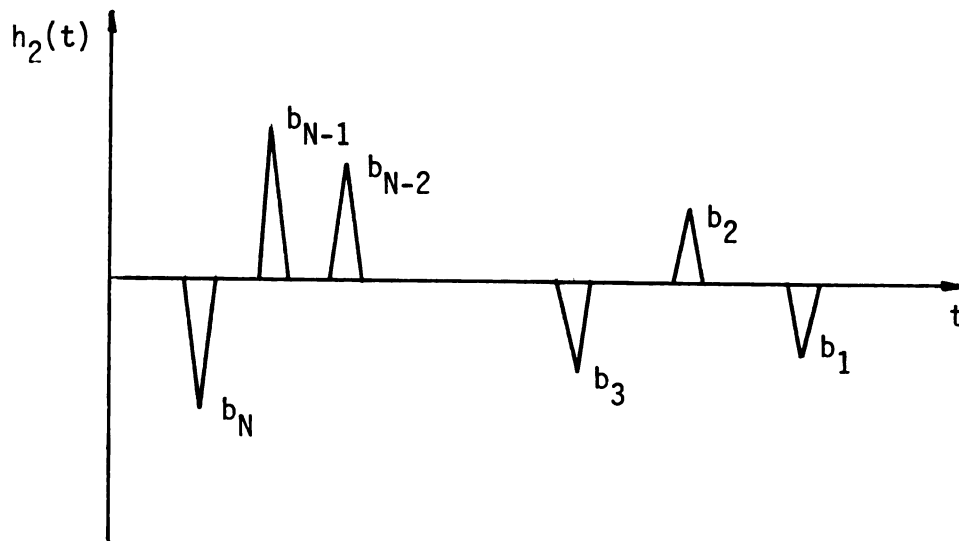
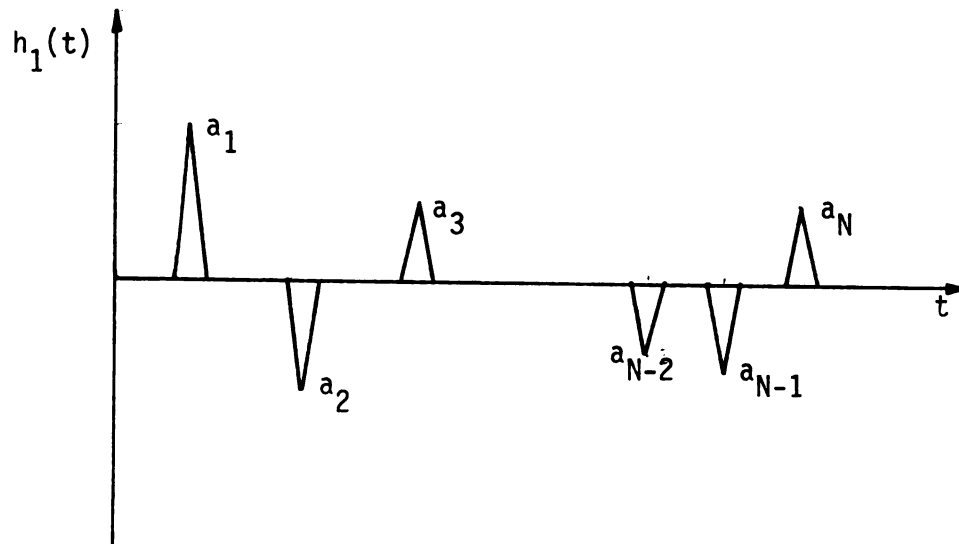


FIGURE 4.3 Bi-directional impulse response functions of a layered object.

$\exp(-2\alpha_i T_i) =$  loss factor - the total loss when the signal propagates forward and backward in the layer bounded by  $i$  th and  $i+1$  st interfaces.

Equations (4.2.6) through (4.2.12) and either the equation (4.2.4) or equation (4.2.5) are sufficient to find the variation of attenuation and impedance along the path of propagation. Hence it is possible to find the variation of attenuation in two ways - using equations (4.2.4) and (4.2.6) through (4.2.12) or equations (4.2.5) through (4.2.12). The results obtained using both sets of equations are given in section 4.3.

### 4.3 EXPERIMENTAL RESULTS

Two models were investigated using the method outlined in section 4.2. The first object to be tested was a symmetrical structure of three layers. The second was a five layered structure. The results obtained are also compared with the values obtained by direct measurement of parameters.

#### 4.3.1 A THREE LAYERED STRUCTURE

The first model to be used in the experiment is shown in Figure 4.4. It consisted of three layers - a machine oil layer separated from water by two acrylic cast (plexi glass) layers. The incident signal waveform, its frequency spectrum and the Hanning filter function used in the calculation are shown in Figures 4.5 and 4.6. As this is a symmetrical structure, it was interrogated only from one side. The corresponding reflected signal is shown in Figure 4.7.

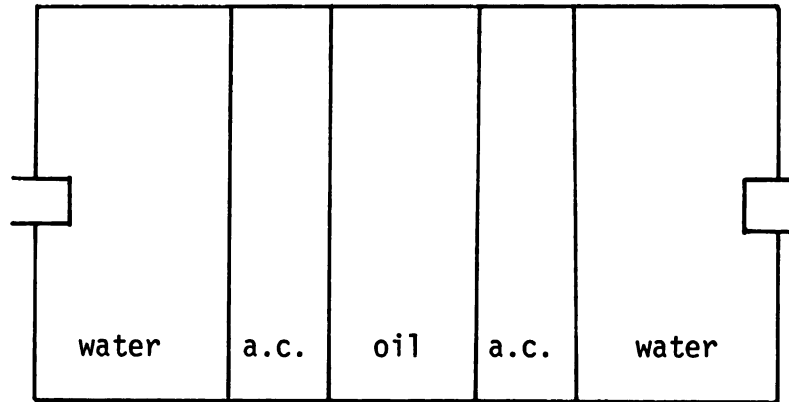


FIGURE 4.4 Test object 1.

The direct impulse response function calculated using the Hanning window of Figure 4.6, before and after amplitude detection are given in Figure 4.8.

The impulse response function obtained using the frequency restored method is given in Figure 4.9. For this purpose, frequency components up to 7.27 MHz were estimated. The Hanning filter function shown in Figure 4.6 was used to weight the original and estimated frequency components. The algorithm used for this purpose is given in Appendix B. One iteration was made. The results obtained using each method are given in Tables 4.1 and 4.2. Table 4.3 gives the results obtained by direct measurement of parameters.



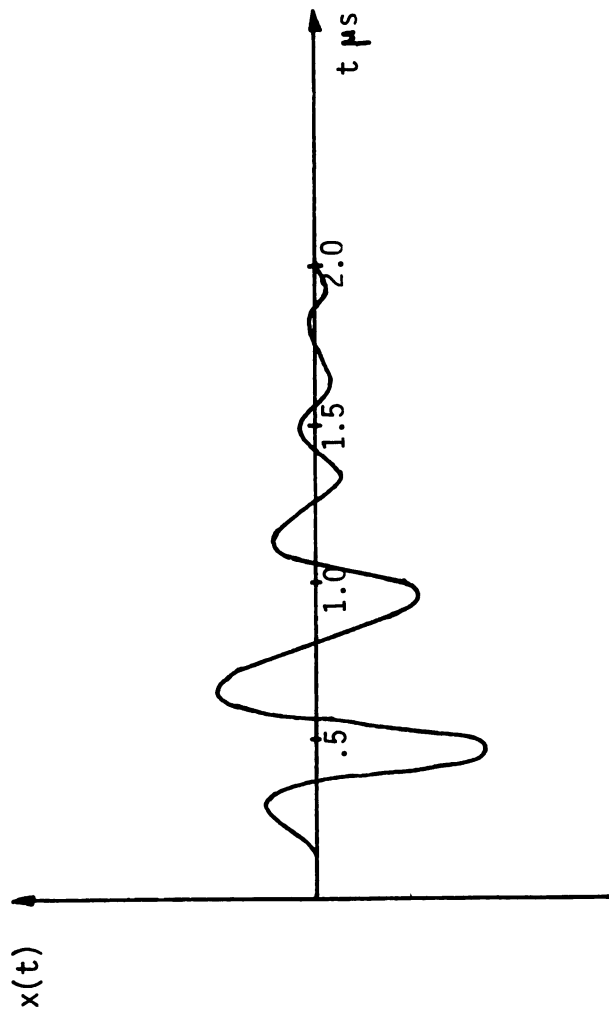


FIGURE 4.5 Incident waveform.

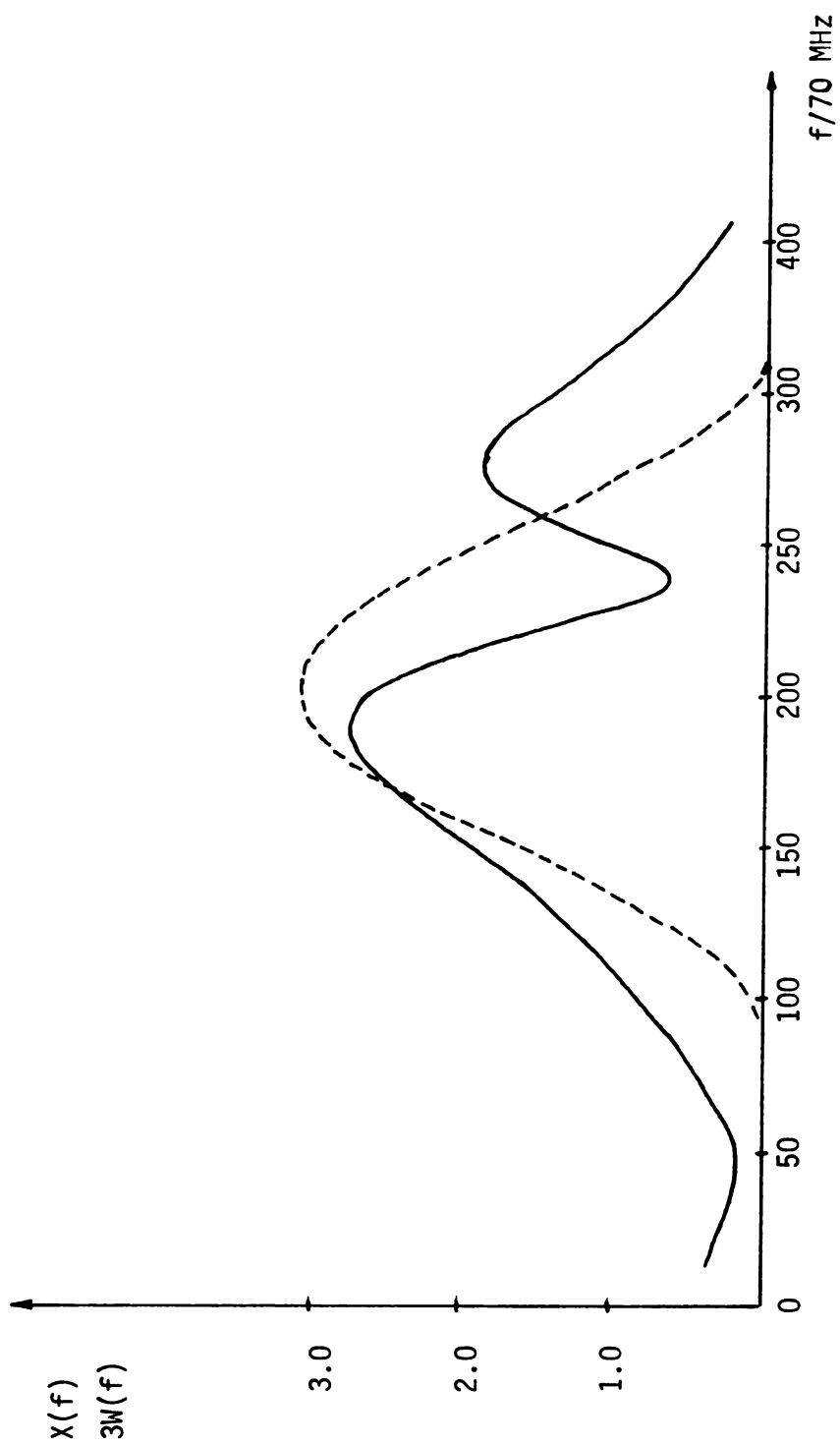


FIGURE 4.6 Incident spectrum and the Hanning filter.

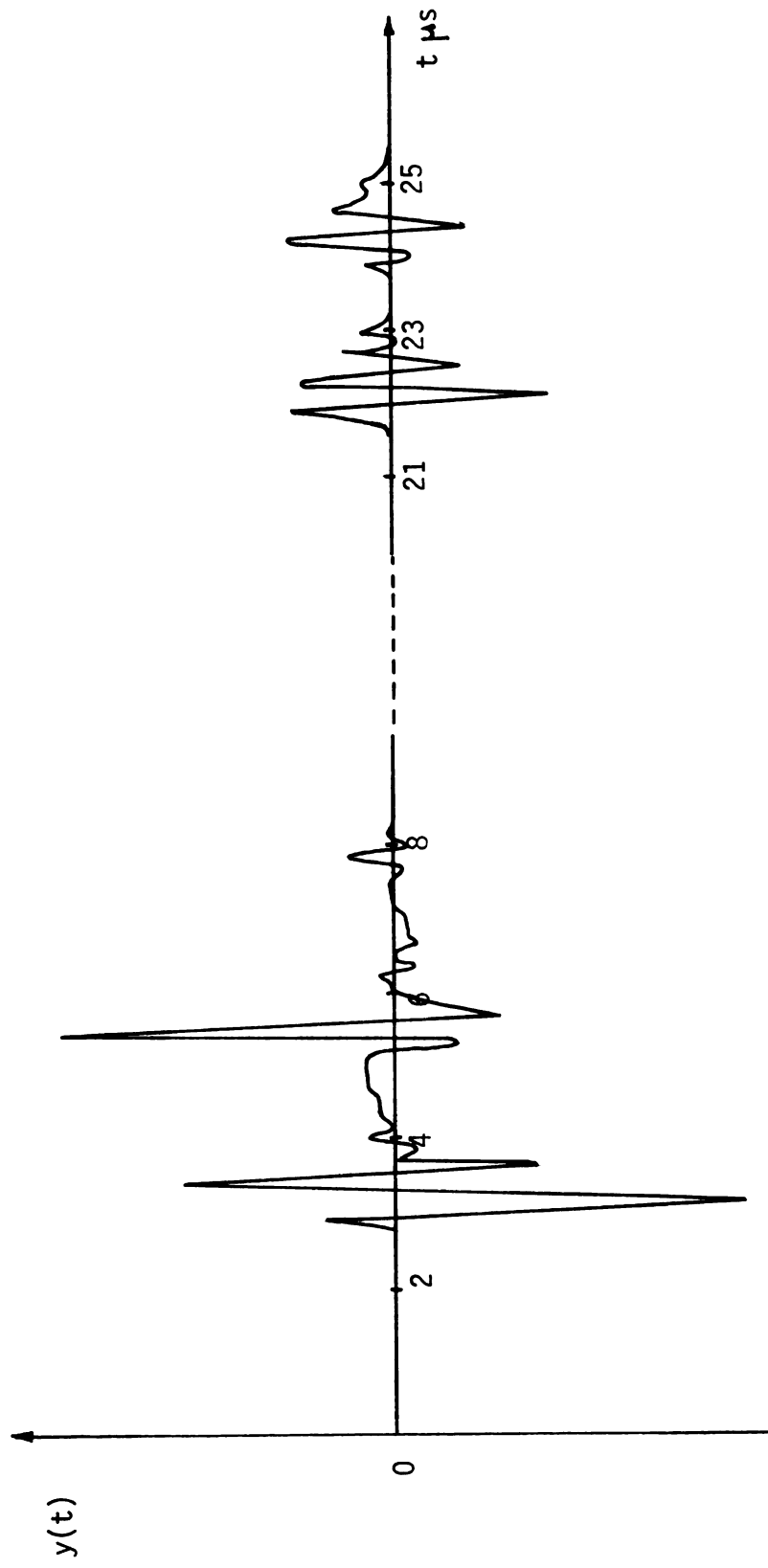


FIGURE 4.7 Reflected waveform.

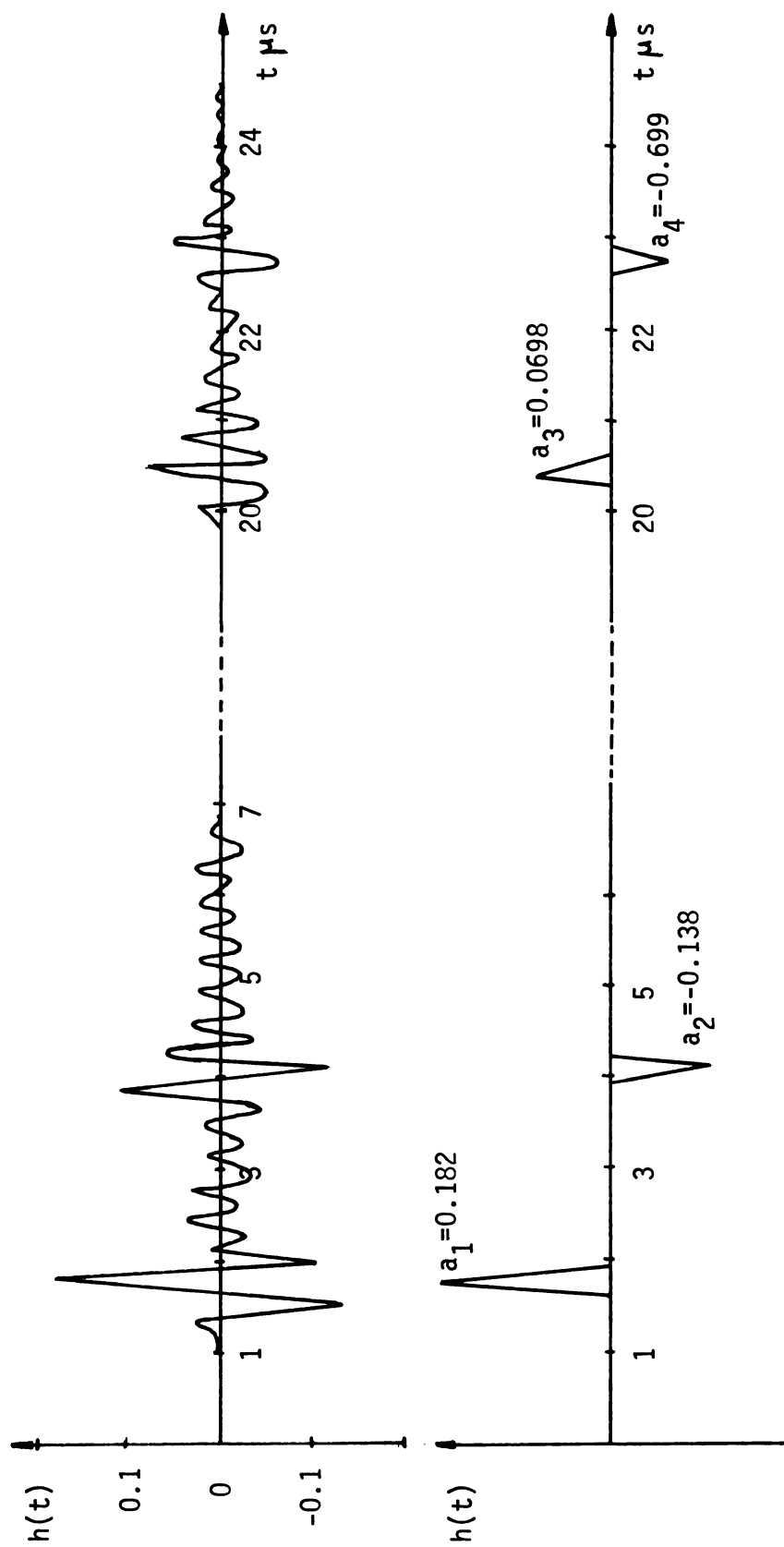


FIGURE 4.8 Direct impulse response function of test object 1 - before and after amplitude detection.

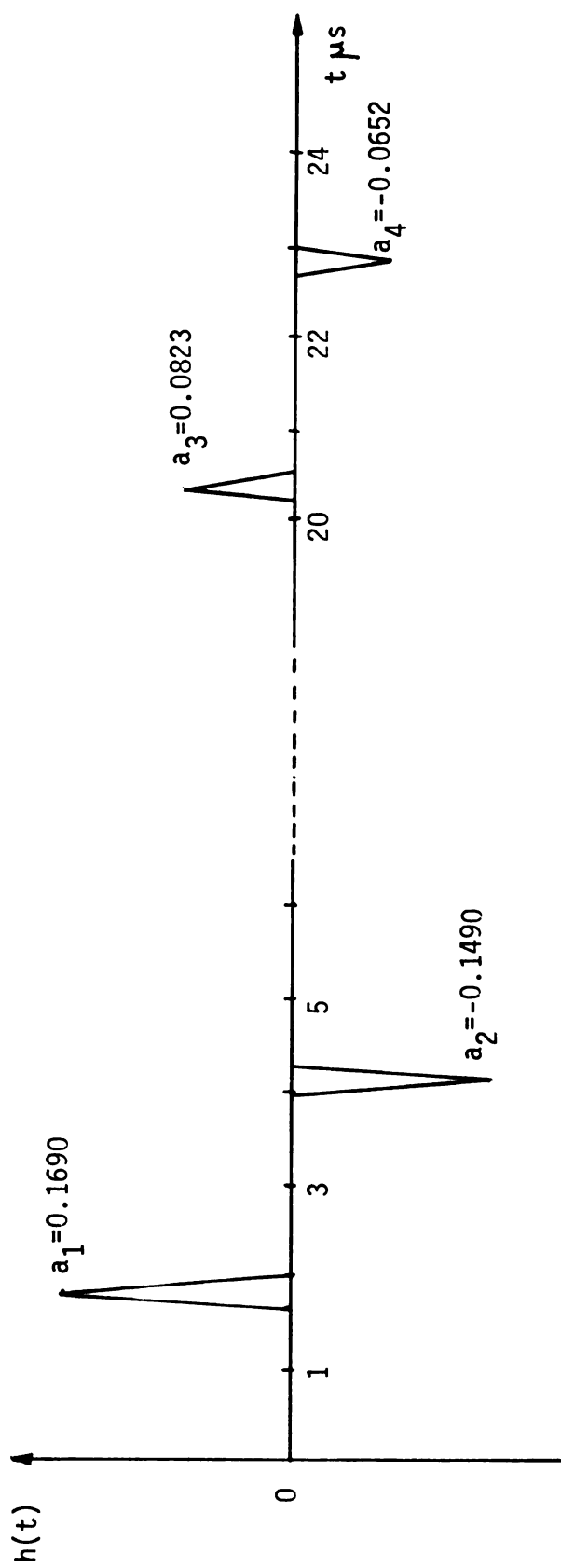


FIGURE 4.9 Frequency restored impulse response function of test object 1.

TABLE 4.1 Results for test object 1 - using direct i.r.f.

## a. Reflection coefficients

Interface	Reflection coefficient
Water / Acrylic cast	0.1820
Acrylic cast / Oil	- 0.1590
Oil / Acrylic cast	0.1590
Acrylic cast / Water	- 0.1820

## b. Layer parameters

Layer	Normalized impedance	Loss factor	Attenuation coefficient (Np/s)
Water	1.00	1.0000	0.0000
Acrylic cast	1.45	0.8976	0.0448
Oil	1.05	0.5189	0.0198
Acrylic cast	1.45	0.8976	0.0448
Water	1.00	1.0000	0.0000

TABLE 4.2 Results for test object 1 - using restored i.r.f.

## a. Reflection coefficients

Interface	Reflection coefficient
Water / Acrylic cast	0.1690
Acrylic cast / Oil	- 0.1774
Oil / Acrylic cast	0.1774
Acrylic cast / Oil	- 0.1690

## b. Layer parameters

Layer	Normalized impedance	Loss factor	Attenuation coefficient (Np/s)
Water	1.00	1.0000	0.0000
Acrylic cast	1.41	0.8589	0.0633
Oil	0.98	0.5739	0.0168
Acrylic cast	1.41	0.8589	0.0633
Water	1.00	1.0000	0.0000

TABLE 4.3 Layer parameters for test object 1 from direct measurements.

Material	Normalized impedance*	Attenuation coefficient (Np/s)
Acrylic cast	1.50	0.13 - 0.18
Oil	0.79	0.0145

\* Normalized with respect to impedance of water.

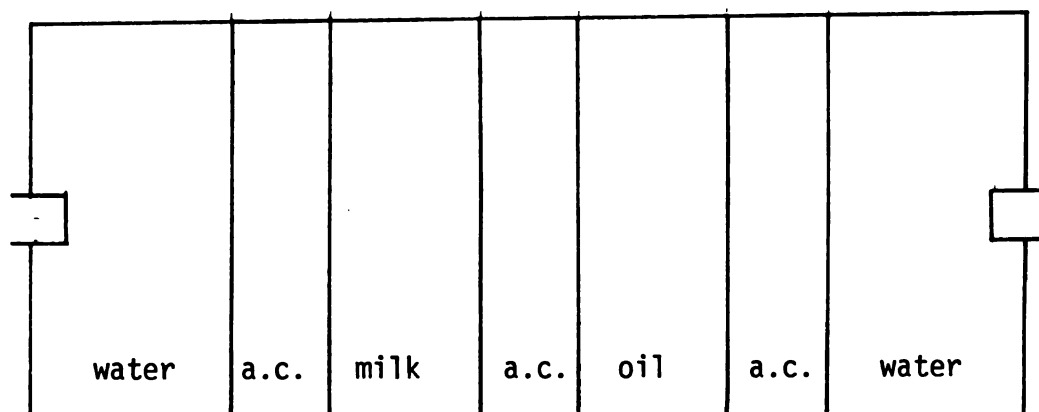


FIGURE 4.10 Test object 2.



#### 4.3.2 A FIVE LAYERED ASYMMETRICAL STRUCTURE

The model shown in Figure 4.10 was the second object to be used in the experiment. It consisted of five layers - three layers of acrylic cast, a layer of milk and a layer of machine oil. The oil used here was different from the one used in the test object 1.

Test object 2 was interrogated using ultrasonic pulses from sides A and B. The corresponding direct and frequency restored impulse response functions are given in Figures 4.11 and 4.12 respectively. The Hanning window used in this experiment is given by,

$$W(f) = \begin{cases} \cos^2 \frac{\pi(f-2.85)}{3.14} & 1.28 < f < 4.42 \\ 0 & \text{otherwise} \end{cases}$$

where  $f$  is the frequency in MHz.

In the frequency restoring method of calculating the impulse response function, frequency components up to 7.85 MHz were estimated. The impulse response function obtained by each method was used to calculate the attenuation and impedance variations in the two ways outlined in section 4.2. The corresponding results are tabulated in Tables 4.4 through 4.7.

It is seen that when equation (4.2.4) is used, the accuracy of the results become less for the layers closer to the B end. Similarly, the accuracy of the results for layers near the A end decreases if  $r_N = -b_N$  - equation (4.2.5) - is used. This is to be expected since the signal to noise ratio is less for the reflections from the far end of the object. Hence the two sets of results can be combined to give more accurate values by using the parameters of

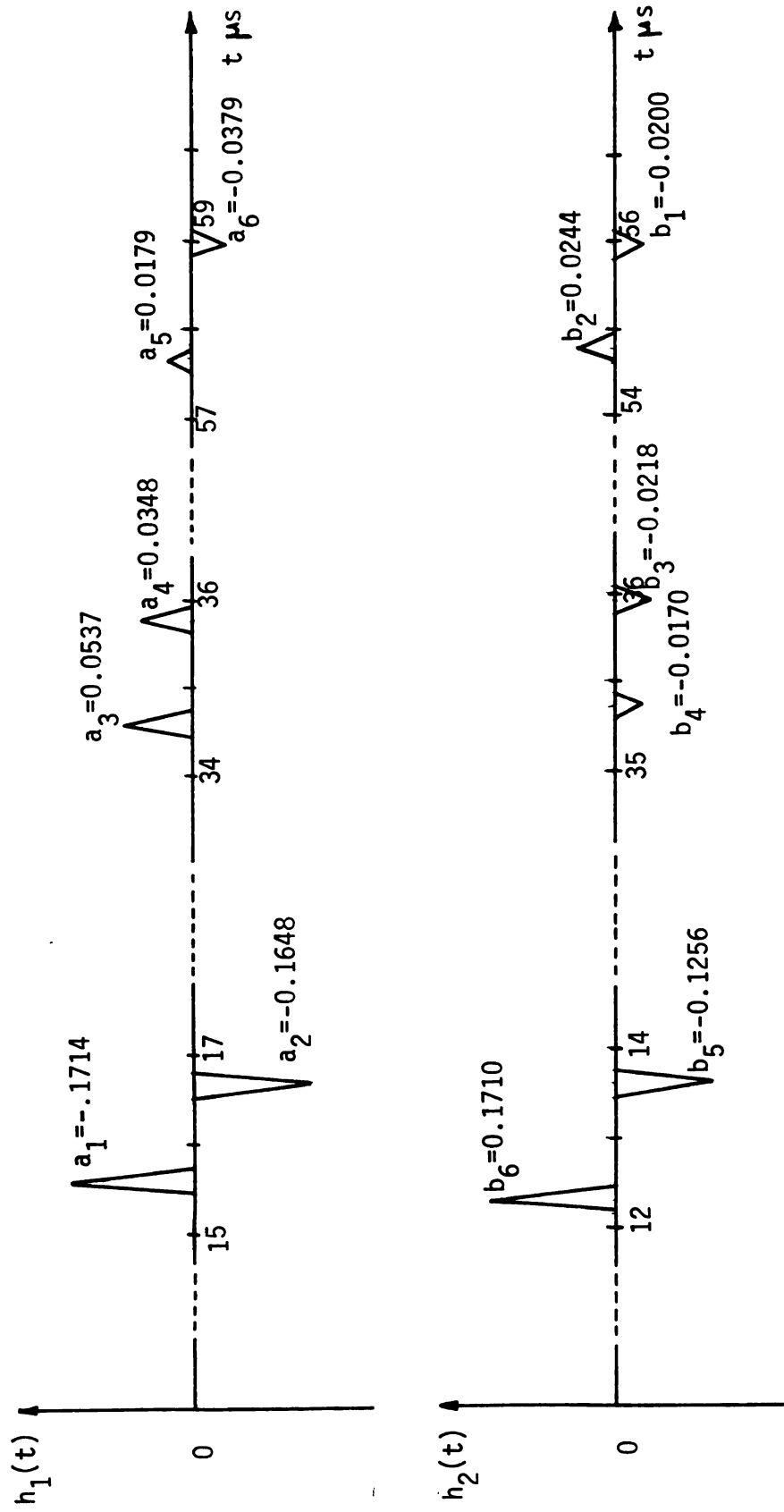


FIGURE 4.11 Bi-directional direct impulse response functions of test object 2.

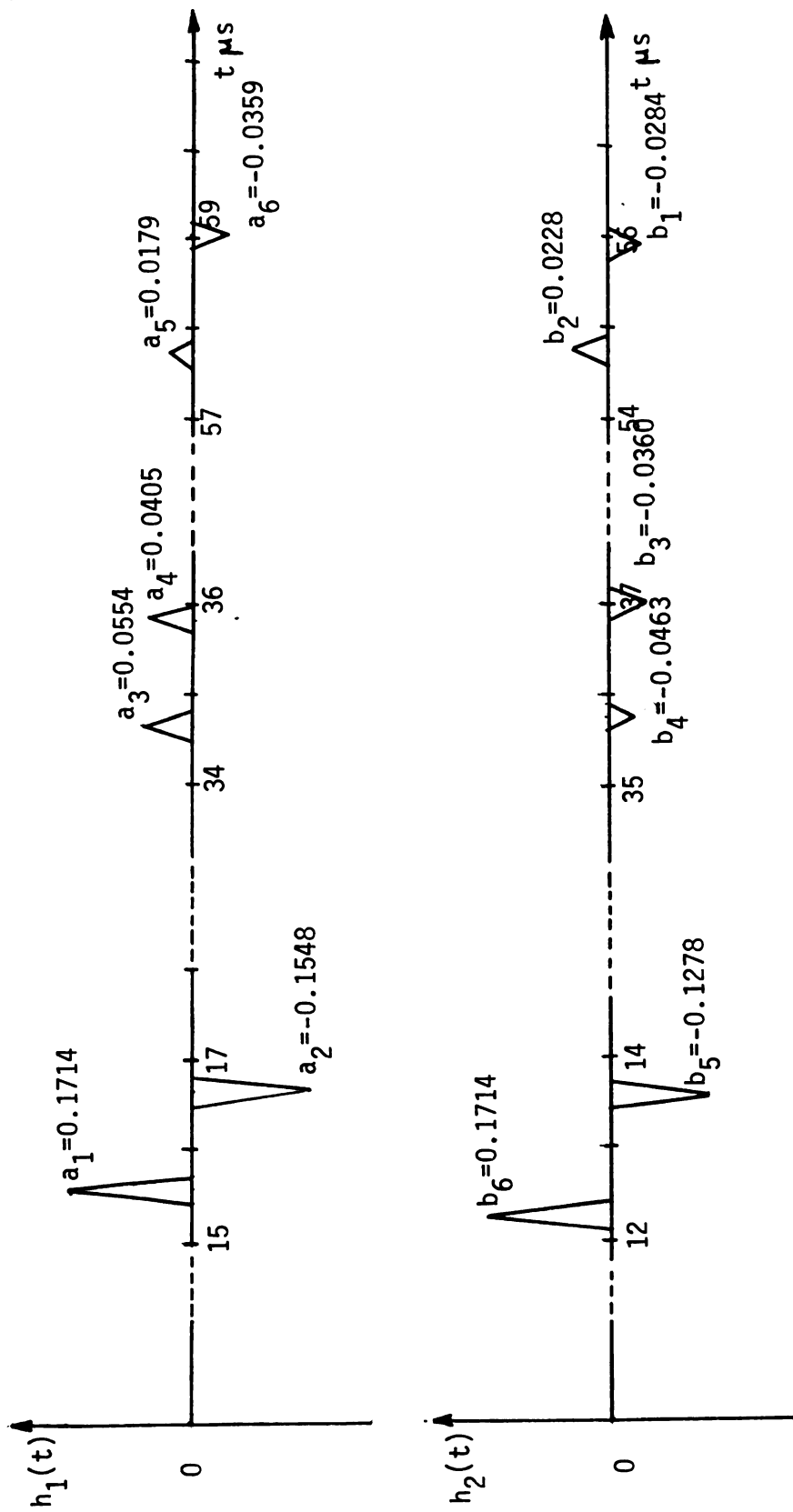


FIGURE 4.12 Bi-directional frequency restored impulse response functions of test object 2.

TABLE 4.4 Results for test object 2 - using direct i.r.f. and

$$r_1 = a_1.$$

## a. Reflection coefficients

Interface	Reflection coefficient
Water / Acrylic cast 1	0.171
Acrylic cast 1 / Milk	- 0.185
Milk / Acrylic cast 2	0.101
Acrylic cast 2 / Oil	0.072
Oil / Acrylic cast 3	0.139
Acrylic cast 3 / Water	- 0.232

## b. Layer parameters

Layer	Normalized impedance	Loss factor	Attenuation coefficient (Np/s)
Water	1.00	1.0000	0.0000
Acrylic cast 1	1.41	0.9185	0.0708
Milk	0.97	0.6173	0.0201
Acrylic cast 2	1.19	0.9160	0.0730
Oil	1.38	0.2679	0.1090
Acrylic cast 3	1.82	1.0000	0.0000
Water	1.13	1.0000	0.0000

TABLE 4.5 Results for test object 2 - using direct i.r.f. and

$$r_6 = -b_6.$$

## a. Reflection coefficients

Interface	Reflection coefficient
Water / Acrylic cast 3	0.171
Acrylic cast 3 / Oil	- 0.102
Oil / Acrylic cast 2	- 0.052
Acrylic cast 2 / Milk	- 0.073
Milk / Acrylic cast 1	0.136
Acrylic cast 1 / Water	- 0.125

## b. Layer parameters

Layer	Normalized impedance	Loss factor	Attenuation coefficient (Np/s)
Water	1.00	1.0000	0.0000
Acrylic cast 3	1.41	1.0000	0.0000
Oil	1.15	0.2664	0.1100
Acrylic cast 2	1.04	0.9127	0.0760
Milk	0.89	0.6108	0.0206
Acrylic cast 1	1.18	0.9047	0.0830
Water	0.91	1.0000	0.0000

---

TABLE 4.6 Results for test object 2 - using restored i.r.f. and

$$r_1 = a_1.$$

## a. Reflection coefficients

Interface	Reflection coefficient
Water / Acrylic cast 1	0.171
Acrylic cast 1 / Milk	- 0.147
Milk / Acrylic cast 2	0.111
Acrylic cast 2 / Oil	0.107
Oil / Acrylic cast 3	0.118
Acrylic cast 3 / Water	- 0.192

## b. Layer parameters

Layer	Normalized impedance	Loss factor	Attenuation coefficient (Np/s)
Water	1.00	1.0000	0.0000
Acrylic cast 1	1.41	1.0000	0.0000
Milk	1.05	0.4843	0.0302
Acrylic cast 2	1.31	0.7630	0.2250
Oil	1.63	0.4053	0.0752
Acrylic cast 3	2.06	1.0000	0.0000
Water	1.40	1.0000	0.0000

TABLE 4.7 Results for test object 2 - using restored i.r.f. and

$$r_6 = -b_6.$$

## a. Reflection coefficients

Interface	Reflection coefficient
Water / Acrylic cast 3	0.171
Acrylic cast 3 / Oil	- 0.106
Oil / Acrylic cast 2	- 0.096
Acrylic cast 2 / Milk	- 0.098
Milk / Acrylic cast 1	0.131
Acrylic cast 1 / Water	- 0.153

## b. Layer parameters

Layer	Normalized impedance	Loss factor	Attenuation coefficient (Np/s)
Water	1.00	1.0000	0.0000
Acrylic cast 3	1.41	1.0000	0.0000
Oil	1.14	0.4042	0.0754
Acrylic cast 2	0.94	0.7611	0.2220
Milk	0.77	0.4826	0.0304
Acrylic cast 1	1.01	1.0000	0.0000
Water	0.74	1.0000	0.0000

TABLE 4.8 Results for test object 2 - using direct i.r.f.

## a. Reflection coefficients

Interface	Reflection coefficient
Water / Acrylic cast 1	0.171
Acrylic cast 1 / Milk	- 0.185
Milk / Acrylic cast 2	0.101
Oil / Acrylic cast 2	- 0.052
Acrylic cast 3 / Oil	- 0.102
Water / Acrylic cast 3	0.171

## b. Layer parameters

Layer	Normalized impedance	Loss factor	Attenuation coefficient (Np/s)
Water	1.00	1.0000	0.0000
Acrylic cast 1	1.41	0.9185	0.0708
Milk	0.97	0.6173	0.0201
Acrylic cast 2	1.19	0.9127	0.0760
Oil	1.15	0.2664	0.1100
Acrylic cast 3	1.41	1.0000	0.0000
Water	1.00	1.0000	0.0000



TABLE 4.9 Results for test object 2 - using restored i.r.f.

## a. Reflection coefficients

Interface	Reflection coefficient
Water / Acrylic cast 1	0.171
Acrylic cast 1 / Milk	- 0.147
Milk / Acrylic cast 2	0.111
Oil / Acrylic cast 2	- 0.096
Acrylic cast 3 / Oil	- 0.106
Water / Acrylic cast 3	0.171

## b. Layer parameters

Layer	Normalized impedance	Loss factor	Attenuation coefficient (Np/s)
Water	1.00	1.0000	0.0000
Acrylic cast 1	1.41	1.0000	0.0000
Milk	1.05	0.4843	0.0302
Acrylic cast 2	1.31	0.7630	0.2250
Oil	1.14	0.4042	0.0754
Acrylic cast 3	1.41	1.0000	0.0000
Water	1.00	1.0000	0.0000

the layers closer to side A from the set of results obtained by assuming  $r_1 = a_1$  and the parameters of the layers closer to side B from the set of results obtained by assuming  $r_N = -b_N$ . These results are given in Tables 4.8 and 4.9. The parameters obtained by direct measurements are given in Table 4.10.

TABLE 4.10 Layer parameters for test object 2 from direct measurements.

Material	Normalized impedance*	Attenuation coefficient (Np/s)
Acrylic cast 1,2,3	1.50	0.1300 - 0.1800
Oil	1.03	0.0350 - 0.0440
Milk	0.98	0.0147 - 0.0217

\* Normalized with respect to impedance of water.

## CHAPTER V

### CONCLUSION

The conventional ultrasound imaging systems make use of the amplitude information of the reflected or transmitted signals. Recent research has resulted in impediography techniques, where the impedance of the medium, derived from the reflected signal, rather than the amplitude of the returned echoes is used as the imaging parameter. The impediographic methods make use of the frequency, phase and amplitude information available in the reflected signal. However, there are some cases, such as imaging of the brain, where the attenuation coefficient would be a better imaging parameter than the impedance. Research has begun very recently on the use of the ultrasound attenuation coefficient as the imaging parameter. The aim of this study was to develop such a method. None of the research, that we came across in this area use reflection techniques. Transmission techniques appear to be an obvious choice in this case, because a signal transmitted through an object contains information about the total attenuation along the path it has travelled. This thesis has investigated a method which uses a reflection technique for ultrasound attenuation imaging. Only one dimensional images - A mode - has been considered. But this can easily be extended to two or three dimensions.

When an ultrasonic pulse gets reflected from an internal discontinuity of an object, the resulting echo is determined by the reflection coefficient at the interface as well as the attenuation of the substances in between the transducer and the reflecting point. The

reflection coefficient is a function of the change in impedance. These two types of information - attenuation and impedance variation along the path of propagation - contained in the reflected signal cannot be separated by the knowledge of reflected signal alone. The additional information necessary to separate the two types of information is derived from another reflected signal. This second reflected signal is obtained by a transmission from the opposite side of the object. This thesis has developed analytical expressions which would allow the separation of information about attenuation and reflection coefficients or the impedance. As a result, the method outlined can extract both the variation of attenuation coefficient and the variation of impedance along the path of propagation. The variation of impedance obtained by this technique should be more accurate than the conventional ultrasonic impediography methods, because those methods neglect the attenuation in the medium, whereas the method outlined in this thesis takes into account the ultrasonic attenuation along the path of propagation. As a matter of fact, the development of an imaging technique utilizing the attenuation coefficient variation is the main concern of this research work.

For the purpose of separating the two types of information - ultrasonic attenuation variation and the impedance variation along the path of propagation - the object under investigation was assumed to have one of the two forms. First, it was assumed that the body has a layered structure, which consists of homogeneous layers. Later this was extended to an inhomogeneous medium having a continuous variation of impedance. The expressions developed for a

layered structures were put to test by using models composed of machine oil, milk and acrylic cast.

The experimental results show that this method has not been able to determine the absolute attenuation coefficients of the internal material accurately. But this does not hamper its ability to be used as an imaging technique, where the relative attenuation coefficient is needed rather than the absolute attenuation coefficient.

The main factor which governs the accuracy of the result is the nonlinear beam spreading of the acoustic wave. This could cause the apparent acoustic attenuation coefficient to be varied along the path of propagation even in a homogeneous object.

This method of determining the attenuation coefficient has the advantage of suppressing the multiple reflections of the returned signal. The reason is that the impulse response function obtained from either side of the object is more accurate for reflections closer to the surface. This is because the power and hence the signal to noise ratio is less for reflected echoes from the deep lying parts of the object. But the deep lying parts of the object for one impulse response function are the near parts of the object for the other impulse response function. Thus, by comparing the time intervals between echoes of the two impulse response functions, the echoes due to multiple reflections and noise can be detected and subsequently suppressed.

The analytical expressions developed for the inhomogeneous case have not been experimentally verified. This has been an extension of the work done on the layered structures. More experiments are needed to establish its validity.

This method heavily depends on the ability to determine the impulse response function accurately. The accuracy of the impulse response function in turn depends on the bandwidth of the transducer. Although techniques have been developed to determine the impulse response function using a narrow band source, a wider transducer bandwidth will certainly improve the accuracy. But too wide a bandwidth can give rise to another problem. The attenuation coefficient for biological matter has been found to be dispersive in the frequency domain. Thus a large bandwidth may result in nonuniform attenuation of various frequency components, which in turn would invalidate the assumptions made in this method. Hence, a bandwidth, which makes it possible to determine the impulse response function accurately, to retain the range resolution within desired limits and at the same time does not cause too much variation of attenuation in the frequency band used has to be selected.

By using methods such as pseudo random binary sequences, the accuracy of the impulse response function may be improved. As this method allows the use of a higher average power, a considerable improvement in signal to noise ratio can be expected. Such methods, which improve the accuracy of the impulse response function, may make this method very attractive in the future developments.

## APPENDICES

## APPENDIX A

### ALGORITHM FOR DIRECT IMPULSE RESPONSE FUNCTION CALCULATION

The algorithm given below is used to calculate the direct impulse response function using the incident and reflected waveforms. The following notation is used.

$x$	=	$x_i$ ; $i=1,2,\dots N$	* Incident signal samples**
$y$	=	$y_i$ ; $i=1,2,\dots N$	Reflected signal samples
$h$	=	$h_i$ ; $i=1,2,\dots N$	Impulse response samples
$X$	=	$X_i$ ; $i=1,2,\dots N$	Discrete Fourier Transform (DFT) of $x$
$Y$	=	$Y_i$ ; $i=1,2,\dots N$	Discrete Fourier Transform (DFT) of $y$
$H$	=	$H_i$ ; $i=1,2,\dots N$	Discrete Fourier Transform (DFT) of $h$
$W$	=	$W_i$ ; $i=1,2,\dots N$	Hanning filter function
$A$	=	$a_i$ ; $i=1,2,\dots k$	Peak values of the impulse response function
$T$	=	$t_i$ ; $i=1,2,\dots k$	Epoch times corresponding to peak values of the impulse response function.

\*  $N$  is selected such that there are adequate number of zeroes on either side of the signal samples to prevent aliasing.

\*\* The duration of the incident signal is very small compared to that of the reflected signal. Hence there are only a small number of non zero samples in  $x$ .



x and y are the data collected in the experiment. This algorithm calculates the sample values  $h_i$  of the impulse response function and detects its peaks by using the amplitude detection scheme given in Appendix C. FFTCC routine resident in the Hustler Auxiliary Library, was used to determine the Discrete Fourier Transform and the Inverse Discrete Fourier Transform. This as well as the other algorithms were implemented using the Cyber machine at the Michigan State University. The algorithm is as follows.

1. Calculate the DFT X of the incident signal samples x.
2. Calculate the DFT Y of the reflected signal samples y.
3. Calculate the filter function W given by

$$w_i = \cos^2 \frac{\pi(i - i_0)}{2\Delta i} \quad \text{for } i_0 - \Delta i < i < i_0 + \Delta i \\ \text{and } N+2-i_0-\Delta i < i < N+2-i_0+\Delta i$$

$$w_i = 0 \quad \text{otherwise}$$

where  $i_0$  is the centre frequency of the incident signal spectrum and  $\Delta i$  is its bandwidth.

4. Calculate the transfer function H given by

$$H_i = W_i \frac{Y_i}{X_i}$$

5. Find the inverse DFT of H, h. h is the direct impulse response function.
6. Call amplitude detection algorithm (Appendix C) for determination of peak values and epoch times.

## APPENDIX B

### ALGORITHM FOR FREQUENCY RESTORED IMPULSE RESPONSE FUNCTION CALCULATION

The algorithm given below is used to calculate the frequency restored impulse response function using the incident and reflected signal samples. The notation given in Appendix A applies here too. The algorithm is as follows.

1. Follow the algorithm for direct impulse response function calculation .
2. If the original bandwidth of the spectrums of  $x, y$  and  $h$ , given by  $(2N\Delta t)^{-1}$  where  $(\Delta t)$  is the sampling time, is sufficient for restoration then go to step 7.
3. Find  $N'$  such that the required bandwidth is given by  $(2N'\Delta t)^{-1}$ .

4. Let

$$H_i = 0 \quad \text{for } i = \frac{N+1}{2}, \dots, N'$$

5. Let

$$H_i = \text{Conjugate}(H_i) \quad \text{for } i = \frac{N'+1}{2}, \dots, N'$$

6. Let

$$N = N'$$

7. From step 1, the positions of the impulses and their magnitude estimates are known. These values are now used to estimate the unreliable frequency components.

a. Form  $P_i$ ,  $i = 1, 2, \dots, N$ , where

$$P_i = \sum_{j=1}^k a_j \exp(-2\pi j \cdot i \cdot t_j / N \cdot \Delta t)$$

b. Form the new estimate of the transfer function

$$H_i = H_i + (1 - W_i) P_i \quad i=1,2,\dots,N$$

8. Find the inverse DFT of the transfer function  $H$ . This is the improved impulse response function.
9. Call the amplitude detection algorithm (Appendix C) to find the improved estimates of echo magnitudes and epoch times.
10. Steps 2 through 9 may be repeated if more accuracy is needed.

## APPENDIX C

### ALGORITHM FOR SOFTWARE IMPLEMENTED AMPLITUDE DETECTION SCHEME

This algorithm is used to detect the peak values and the corresponding epoch times of the impulse response function. This is not similar to any hardware implemented amplitude detection scheme. The input to the algorithm is in the form of a sequence  $h_i$ ,  $i=1,2,\dots,N$ , where  $h_i$  are the sample values of the impulse response function calculated using the algorithms given in Appendices A and B. The output is in the form of two sequences  $a_j$  and  $t_j$ ,  $j=1,2,\dots,k$ .  $a_j$  is the  $j$ th peak value detected and  $t_j$  is its position in time. The algorithm is given by the flow diagram shown in Figure A.1.

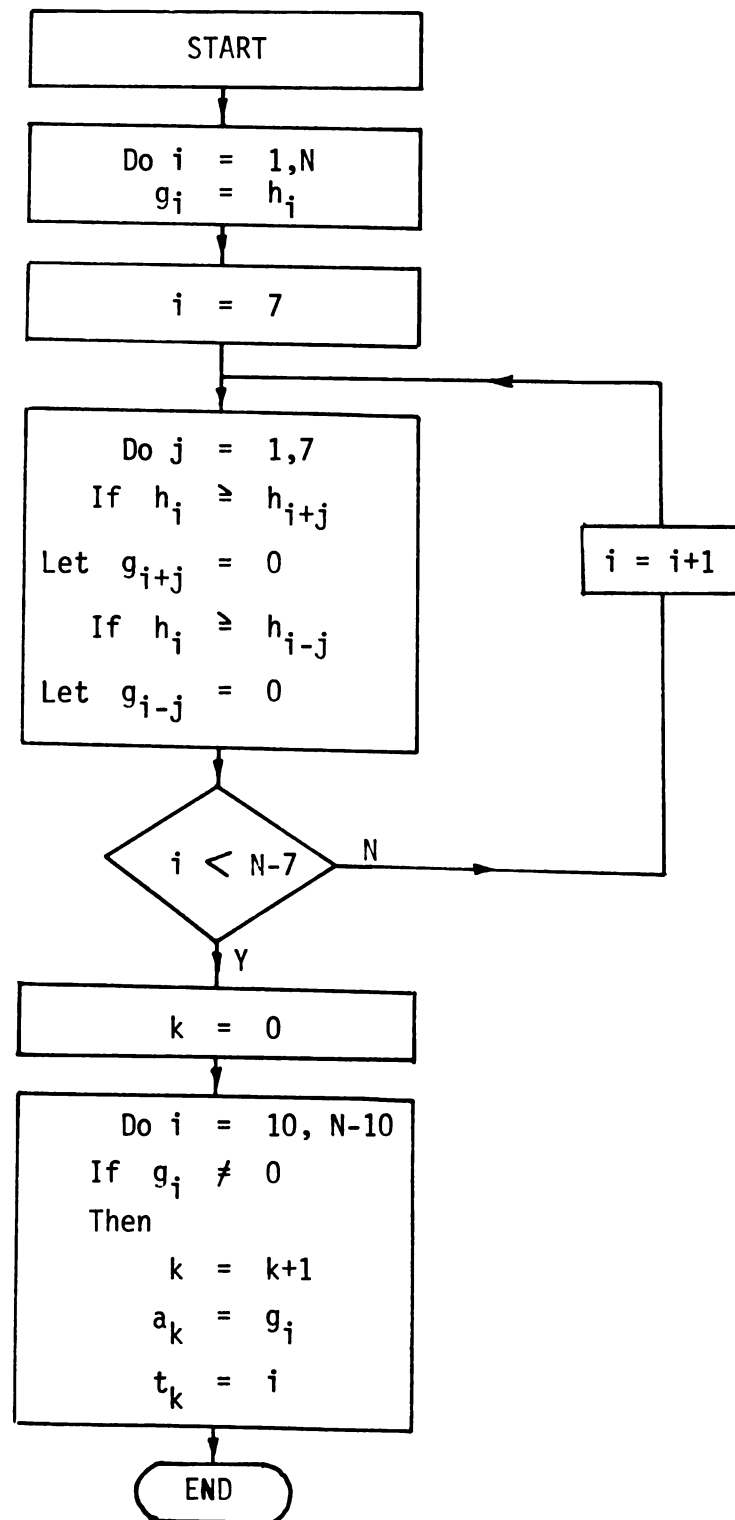


FIGURE A.1 Flow diagram of the amplitude detection scheme.

## BIBLIOGRAPHY

1. Beretsky, I. , "Detection and characterization of Atherosclerosis in a human arterial wall by Raylographic technique, an in-vitro study", Ultrasound in Medicine, Volume 3B, Plenum Press, 1977.
2. Beretsky, I. , Farrell, G. , Lichtenstein, B. , "Raylography, A pulse echo technique with future biomedical applications", Proceedings of the 20 th Annual Meeting of the American Institute of Ultrasound in Medicine, 1976.
3. Beretsky, I. , "Raylography, A frequency domain processing technique for pulse echo ultrasonography", Ultrasound in Medicine, Volume 3B, Plenum Press, 1977.
4. Beretsky, I. , Farrell, G. , "Improvement of ultrasonic imaging and media characterization by frequency domain deconvolution, experimental study with nonbiological models", Ultrasound in Medicine, Volume 3B, Plenum Press, 1977.
5. Fourcade, C. , Cathignol, D. , Chapelon, J.Y. , "A new pseudo Random binary code phase modulated ultrasonic high resolution Echograph", 4 th International Symposium on Ultrasonic Tissue Characterization, N.B.S., 1979.
6. Frizzell, L.A. , "Shear properties of mammalian tissues at low megahertz frequencies", J. Acoustic Society of America, Volume 60, No. 6, December 1976.
7. Fry, W.J. , "Mechanisms of acoustic absorption in tissue", J. Acoustic Society of America, Volume 24, 1952.
8. Goldman, D.E. , Heuter, T.F. , "Tabular data of the velocity and absorption of high frequency sound in mammalian tissue", J. Acoustic Society of America, Volume 28, 1957.
9. Greanleaf, J.F. , Bahn, R.C. , "Clinical imaging with transmissive ultrasonic computerized tomography", IEEE Trans. on Biomedical Engineering, Volume BME 28, No. 2, 1981.
10. Goss, S.A. , Johnston, R.C. , Dunn, F. , "Comprehensive compilation of empherical ultrasonic properties of mammalian tissue", J. Acoustic Society of America, 1978.
11. Herzfeld, K.F. , Litovitz, A.T. , "Absorption and dispersion of ultrasonic waves", Academic Press, 1959.

12. Jones, J.P. , "Ultrasonic impediography and its applications to tissue characterization", Recent Advances in Ultrasound in Bio-medicine", 1977.
13. Jones, J.P. , "Impediography: A new ultrasonic technique for diagnostic medicine", Ultrasound in Medicine, Volume 1, Plenum Press.
14. Jones, J.P. , "A preliminary experimental evaluation of ultrasonic impediography", Ultrasound in Medicine, Volume 1, Plenum Press.
15. Jones, J.P. , Erikson, R.K. , Fry, F.J. , "Ultrasound in Medicine - A review", IEEE Trans. on Sonics and Ultrasonics, Volume SU 21, No. 3, July 1974.
16. Klepper, J.R. , Brandenburger, G.H. , Mimbs, J.W. , Sobel, B.E. , Miller, J.G. , "Application of phase insensitive detection and frequency dependent measurements to computed ultrasonic attenuation tomography", IEEE Trans. Biomedical Engineering , Volume BME 28, No. 2, February 1981.
17. Kuc, R. , Schwartz, M. , Kaufman, J. "Kalman filtering approach in the analysis of reflected ultrasonic signals", 4 th International Symposium on Ultrasonic Imaging and Tissue Characterization, N.B.S., 1979.
18. Kuc, R. , Schwartz, M. , Von Micsky, L. , "Parametric estimation of the attenuation coefficient for soft tissue", Ultrasonic Symposium Proceedings, 1976.
19. Lichtenstein, B. , Beretsky, I. , Farrell, G. , Winder, A. , "Medium characterization by the application of a deconvolution technique in an acoustic pulse echo system - Raylography", Ultrasound in Medicine, Volume 2.
20. Lizzi, F.L. , Laviola, M.A. , "Power spectrum measurement of ultrasonic backscatter from ocular tissues", Ultrasonic Symposium Proceedings of the IEEE group on Sonics and Ultrasonics, 1975.
21. Lizzi, F.L. , Katz, L. , St.Louis, L. , Coleman, D.J. , "Applications of spectral analysis in medical ultrasonography", Ultrasonics, March 1976.
22. Papoulis, A. , Chamzas, C. , "Improvement of range resolution by spectral extrapolation", 4 th International Symposium on Ultrasonic Imaging and Tissue Characterization, N.B.S., 1979.
23. Papoulis, A. , Beretsky, I. , "Improvement of range resolution of a pulse echo system", Ultrasound in Medicine, Volume 3B, Plenum Press, 1977.

24. Schwan, R. Herman, (Editor), "Biological Engineering", McGraw Hill, 1969.
25. Wells, P.N.T. , "Physical Principles of Ultrasonic Diagnosis", Academic Press, 1969.



MICHIGAN STATE UNIV. LIBRARIES



31293006947133